Chapter 5
Ultrasonic Methods

Vykintas Samaitis, Elena Jasiūnienė, Pawel Packo, and Damira Smagulova

Abstract Ultrasonic inspection is a well recognized technique for non-destructive testing of aircraft components. It provides both local highly sensitive inspection in the vicinity of the sensor and long-range structural assessment by means of guided waves. In general, the properties of ultrasonic waves like velocity, attenuation and propagation characteristics such as reflection, transmission and scattering depend on composition and structural integrity of the material. Hence, ultrasonic inspection is commonly used as a primary tool for active inspection of aircraft components such as engine covers, wing skins and fuselages with the aim to detect, localise and describe delaminations, voids, fibre breakage and ply waviness. This chapter mainly focuses on long range guided wave structural health monitoring, as aircraft components require rapid evaluation of large components preferably in real time without the necessity for grouding of an aircraft. In few upcoming chapters advantages and shortcommings of bulk wave and guided wave ultrasonic inspection is presented, fundamentals of guided wave propagation and damage detection are reviewed, the reliability of guided wave SHM is discussed and some recent examples of guided wave applications to SHM of aerospace components are given.

5.1 Introduction to Ultrasonic Inspection

Ultrasonic inspection is based on interaction (transmission, reflection and absorption) of the mechanical acoustical waves with the analysed structure at frequencies of 20 kHz or above. Conventional bulk wave ultrasonic techniques have been

V. Samaitis (✉) · D. Smagulova
Kaunas University of Technology, Kaunas, Lithuania
e-mail: vykintas.samaitis@ktu.lt

E. Jasiūnienė
Prof. K. Baršauskas Ultrasound Research Institute, Kaunas University of Technology, Kaunas, Lithuania

P. Packo
AGH University of Science and Technology, Krakow, Poland

M. G. R. Sause, E. Jasiūnienė (eds.), *Structural Health Monitoring Damage Detection Systems for Aerospace*, Springer Aerospace Technology,
https://doi.org/10.1007/978-3-030-72192-3_5

extensively used both for material property evaluation and for flaw detection. Material property evaluation is often based either on elastic modulus evaluation by measuring shear and longitudinal wave velocities, or estimation of frequency-dependent attenuation (Sol et al. 2018; Ito et al. 2015; Lin et al. 2011). Both parameters are very commonly used for evaluation of the characteristics and volume of the localized porosity in composites (Duong et al. 2015; Kim et al. 2013; Podymova et al. 2019). Meanwhile, the flaw detection relies on the analysis of surface, back-wall and intermediate echoes within the investigated structure, presuming that any inclusion, delamination or other defect will introduce a reflection that can be captured by the ultrasonic sensor (Zhang et al. 2020a; Hauffe et al. 2020). Because of their relative simplicity, the conventional bulk wave ultrasonic techniques are often used as a primary tool for evaluation of the structural integrity. Ultrasonic C-scan measurement is a common method to assess the structural integrity of composites using bulk ultrasonic waves. Using such technique, the structural response is collected at different spatial positions across the surface of the sample. The output image is usually a colour coded representation of the amplitude level (transmission losses) of the backwall signal. The success of such measurement depends on the type and origin of defects. For example, delamination and debonding defects can produce discrete reflection which can be detected at certain depths before arrival of the backwall signal. Porosity and ply waviness introduce scattering of ultrasonic signal and increased transmission losses (Zhang et al. 2020b; Towsyfyan et al. 2020; Pain and Drinkwater 2013). The multi-layered structure of the composite itself generates structural noise, which complicates the inspection, while the resin layers between the fibres can cause inter-ply reflections and interference of ultrasonic signal. Such interference is known to be stronger when the wavelength of ultrasonic signal is equal to odd number of layer thickness (Zhang et al. 2020a). In case of multiple defects present, a shadowing effect and structural noise generated by layers of composite can limit detectability of some defects, especially in the case of normal incidence inspection.

Aircraft structures may have defects of different type and origin. Some of the defects develop during the manufacturing, while others within the life-cycle of the structure. The most common defects found in aircraft structures are described in Chap. 3 of this book. As the bulk wave measurements are mostly localized, based on point-by-point acquisitions using encoded scanners it's not an ideal choice for large and curved aircraft structures. Classical bulk wave inspection methods are currently used in scheduled maintenance of an aircraft. These methods are able to detect defects in limited area only. Furthermore, they usually require disassembly (to have access to parts, hidden defects) and submersion, are slightly operator-dependent and require to repeat the inspection procedure in different areas of the structure (Hellier 2012; Rocha et al. 2013). As a result, bulk wave inspections are reliable but despite advancements in non-contact measurement methods, yet slow and costly, especially for large engineering structures. The scheduled maintenance requires an aircraft to be grounded so it's usually preferred to perform it as quickly and as rarely as possible. This puts some pressure for fleet operators and increases the risk of

human errors. In the case of large structure inspection, additional challenges arise due to the unreliable contact between the structure and ultrasonic sensor which may appear during the scanning. Conventional bulk wave measurement methods require either the submersion or continuous water feed which limits their applicability on site (Towsyfyan et al. 2020; Ramzi et al. 2015). Special bubblers and water columns are being used then, to provide consistent coupling (Hsu 2013). Air coupled or laser methods enable to partially solve this issue, providing the flexibility to adapt to the complex geometries (Kazys et al. 2017; Pelivanov et al. 2014). However, the impedance mismatch induced losses of air-coupled transducers and expensive equipment of the laser-generated-ultrasound reduces the extent of such approaches.

Current aircraft engineering is trying to implement a "Fail safe" design in which the structure is engineered to maintain the residual strength even in the failure of some structural elements. The scheduled inspection intervals are calculated according to the predicted crack growth rate and loads during the flight (Rocha et al. 2013). In such way it's ensured that an aircraft will be safe to use before another inspection. Such engineering approach suggests that the inspection intervals could be prolonged with the real-time monitoring techniques, that provide defect state information. Hence, in the case of aircraft inspection, an important aspect is to be able to recognize and continuously monitor the development of defects, since it determines the safety of the passengers and would allow to perform condition based maintenance rather than scheduled. This goal can partly be achieved through Structural Health Monitoring (SHM) systems, which aim to inspect large structures in real-time using a distributed network of embedded sensors. The SHM systems usually are not the standalone ones, since they cannot achieve such high measurement accuracy and sensitivity as bulk wave techniques. On the other hand, such approach in contrast to bulk wave inspection does not require prior knowledge about the locations of defects, as it provides global inspection of the structure. As a result, SHM is frequently used to record the response of the structure under the operational loads and to identify and preferably localise the critical regions where the defects may occur. Meanwhile the bulk wave methods usually follow-up the SHM inspection for more precise defect assessment, size evaluation and etc. In most structures, defects are allowed to exist as long as they are considered as safe (Alokita et al. 2019). For a such already known defects, aircraft inspection can benefit from SHM which continuously monitors their development with the aim to capture the moment when they become critical. Typically a successful SHM system should address the challenges and requirements for inspection of aircrafts. These are usually large and thin structures possessing variable geometry which have to be inspected with one-side access. In most cases, inaccessible parts, hidden reinforcement elements and interfaces exist, while the monitoring system should be capable of detecting both defects like delaminations and structural changes i.e. ply waviness, fibre structure etc. This brings a lot of challenges for implementation of successful SHM system.

5.2 Ultrasonic Guided Wave (GW) Inspection

As an alternative to conventional bulk wave ultrasonic inspection, ultrasonic guided waves (GW) emerged as a technique, which enables the implementation of large scale and on-demand SHM systems, through embedded sensor networks (Croxford et al. 2007). As a result, a periodic pointwise inspection can be replaced with real-time long-range condition monitoring, thus minimizing the downtime, human involvement and disassembly of components. Guided waves itself can be defined as a kind of ultrasonic waves that propagate along the boundaries of the structure, or along thin, plate like structural components. It's a result of interference between the longitudinal and shear waves, that propagate back and forth in the analysed structure and conform to the distinct modes (Rose 2002). Guided waves interrogate with the entire bulk of the structure, are sensitive to the changes in elastic modulus or density of the material and are relatively weakly attenuated; hence, defects of different types and positions inside the component can be detected in large structures employing only a few sensors (Cawley 2007). As the velocity and attenuation of guided waves depend on the properties of the material, various sudden changes in the internal structure such as defects can be detected (Kralovec and Schagerl 2020).

Guided waves arise in bounded media as a result of the superposition of bulk waves that are partially transmitted, reflected and refracted at a structure's boundaries and/or internal interfaces. As the focus of this work is on aerospace applications, we are mainly concerned with light thin-walled structures, i.e. plates. In the case of plates, the medium is bounded by two parallel stress-free surfaces, which convert and reflect elastic waves. After multiple reflections, a steady-state pattern is established giving rise to the so-called Lamb waves (Lamb 1917). Lamb waves possess an infinite number of modes of two possible thickness-symmetry types of the displacement field: symmetric (S_i) and anti-symmetric (A_i). There exist additional family of shear horizontal (SH_i) modes, which decouple from S_i and A_i modes for isotropic structures. The subscript ($i = 0, 1 \ldots \infty$) denotes the order of each mode.

Various analysis methods can be employed for calculation of the relationship between wave speed and excitation frequency, i.e. dispersion relationships. For instance, for isotropic, homogeneous, linearly-elastic materials, the dispersion curves can be found using the method of potentials (Viktorov 1967; Rose 2004). Despite its simplicity and mathematical elegance, the method of potentials gives little insight into the physics of the problem. A substantially different approach relies on the partial wave technique (Solie and Auld 1973). Following the latter technique, the first step in formulating the dispersion relationships is the calculation of possible bulk waves for the infinite medium, followed by finding partial waves satisfying stress-free boundary conditions. In addition to dispersion, i.e. phase-frequency relations, the amplitude-frequency characteristics and mode-specific displacement patterns can be found by employing the abovementioned techniques.

Each GW Lamb wave mode has specific dominant displacements; hence, different modes are applied for the detection of particular defects. The anti-symmetric modes possess dominant out-of-plane displacements at low frequencies, therefore

they are commonly used for the detection of delaminations, surface and sub-surface defects (Ramadas et al. 2010; Teramoto et al. 2015). In contrast, symmetrical modes are dominated by in-plane displacements and are widely used for crack and notch assessment (Benmeddour et al. 2009). Such displacement distributions are usually non-uniform across the thickness of the structure and tend to rearrange while frequency-thickness product increases (Rose 2014). The fundamental anti-symmetric modes have a shorter wavelength, leading to a better sensitivity to the defects of small size. Fundamental shear horizontal mode (SH_0) in isotropic media is non-dispersive, so it's frequently employed in various fields intending to avoid complicated signal analysis (Nazeer et al. 2017). The shear horizontal mode has in-plane displacements that are perpendicular to the direction of wave propagation (Rose 2004). Most of the modes of Lamb waves unlike SH_0 are dispersive and display frequency-dependent phase and group velocities. Fundamental 0^{th} order modes usually are fairly non-dispersive at low frequencies and possess quite uniform mode shapes (in-plane and out-of-plane displacements) across the thickness of the sample. Such modes are easily generated and may be a good starting point for any guided wave inspection (Khalili and Cawley 2018; Senyurek 2015). Higher order modes possess relatively short propagation distances due to dispersion, but on the other hand are quite sensitive to small defects due to short wavelength and strong velocity dependence on sample thickness (Masserey et al. 2014; Masserey and Fromme 2015). Hence, the guided wave inspection can be categorized into short to medium and medium to long range.

A typical example of short range inspection can be inspection of aircraft repair patches (Puthillath and Rose 2010; Caminero et al. 2013) and assessment of adhesive bonds (Fromme et al. 2017; Wojtczak and Rucka 2021). Adhesive bonding is frequently used in many aircraft structures to attach wing skins, fuselage stingers and metallic honeycomb to skins for elevators, ailerons, tabs and spoilers (Higgins 2000). Short range guided wave inspection possess relatively minor dispersion, hence the selection of the suitable mode is mostly determined by it's sensitivity. Long range inspection is typically applied for inspection of wing skins, engine coverings and fuselages. In case of long range inspection the dispersion plays a vital role. Due to dispersion various frequency components of the signal travel at different velocities. This leads to a spread of the wave in time domain as it propagates in the structure. Typically for the S_0 mode, the low-frequency components travel faster in comparison to high signal frequencies. In contrast, for A_0 mode high frequencies tend to move more rapidly. As a result, the trail of S_0 mode becomes contracted, while A_0 mode becomes stretched-out (Mitra and Gopalakrishnan 2016). In the presence of dispersion, the velocity of different components of the signal depends on frequency and thickness product. Dispersion is undersirable effect as spreading of wave in time domain reduces the resolution while reduction of the amplitude due to wave spread limits the sensitivity of inspection system (Wilcox et al. 2001a). One of the simpliest way to achieve mode control is to select an appropriate frequency-thickness range where only a few fundamental modes exist. For example, if dispersion diagram shows that only a fundamental modes exist below 1 MHz·mm (see Fig. 5.1), it means that for 10 mm

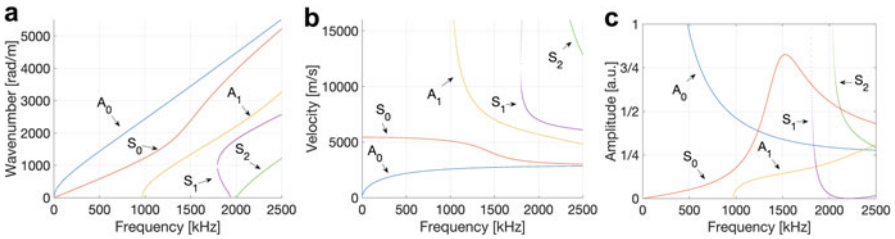

Fig. 5.1 Dispersion ((**a**)—wavenumber-frequency, and (**b**)—velocity-frequency) and out-of-plane excitability (**c**) curves for guided Lamb waves in a 2 mm-thick aluminum plate ($\lambda = 60{,}500$ MPa, $\mu = 25{,}900$ MPa and $\rho = 2700$ kg/m^3)

plate the fundamental modes will propagate at frequencies below 100 kHz. The frequency-thickness product plays vital role in guided wave inspection of aircraft components. These usually posses different complexity of the geometry—from simple plate-like skin elements, to bends and co-cured stiffeners. In such structures the existence of multiple modes becomes unavoidable, while each structural element introduces it's own complexities. For example, stiffeners cause damping of A_0 mode, due to energy leakage into the stiffener and mode conversion which leads to trailing waves. Meanwhile the disbond between skin and stiffener results in a wave propagating in the skin only (Panda et al. 2018). The velocity variation of guided wave modes indicates the thickness change of the structure, which may be caused by different defects, like delamination or disbond or corrosion. To mitigate the effect of dispersion, the bandwidth of the signal for a given plate thickness must be selected carefully, especially for the long-range guided wave applications. Other methods include sparse array excitation which will be discussed in next subchapter. Subsequent sections outline the theoretical background for unbounded and guided wave propagation. As for a linear elastic isotropic medium, guided wave propagation may be considered in a 2-D space, therefore the following discussion is restricted to that simplified case only.

5.2.1 Governing Equations of GW Wave Propagation

5.2.1.1 Waves in Unbounded Media

The momentum equation for a two-dimensional unbounded linear elastic isotropic space is written as

$$\rho \frac{\partial^2 \boldsymbol{X}}{\partial t^2} = \nabla \cdot \boldsymbol{\sigma} \tag{5.1}$$

where ρ denotes the density, $\boldsymbol{X} = [u, v]^T$ the particle displacement vector in 2-D space, $\boldsymbol{\sigma}$ the Cauchy stress tensor and t the time. Equation (5.1), together with constitutive and geometric relationships, fully describes wave motion via particle displacements. For small-amplitude waves, the infinitesimal strain definition is given as

$$\varepsilon_{ij} = \frac{1}{2}\left(\frac{\partial X_i}{\partial D_j} + \frac{\partial X_j}{\partial D_i}\right) \tag{5.2}$$

where X_i denote i^{th} component of the particle displacement vector and D_i represents i^{th} spatial direction. Alternative strain measures may be assumed for small but finite or large strains, e.g. the Green-Lagrange strain tensor (Packo et al. 2016).

For a linear elastic isotropic solid in 2-D, the constitutive relation—linking stresses and strains—yields

$$\sigma_{11} = (\lambda + 2\mu)\varepsilon_{11} + \lambda\varepsilon_{22} \tag{5.3}$$

$$\sigma_{22} = (\lambda + 2\mu)\varepsilon_{22} + \lambda\varepsilon_{11} \tag{5.4}$$

$$\sigma_{12} = 2\mu\varepsilon_{12} \tag{5.5}$$

Combining Eqs. (5.1), (5.2) and (5.3)–(5.5) and assuming the time-harmonic factor $e^{i\omega t}$, the elastodynamic equation yields

$$\rho\omega^2\boldsymbol{X} - \boldsymbol{a_1}\frac{\partial^2\boldsymbol{X}}{\partial x^2} - \boldsymbol{a_2}\frac{\partial^2\boldsymbol{X}}{\partial y^2} - \boldsymbol{a_3}\frac{\partial^2\boldsymbol{X}}{\partial x\partial y} = 0 \tag{5.6}$$

where the matrices $\boldsymbol{a_1}$, $\boldsymbol{a_2}$ and $\boldsymbol{a_3}$ are given by

$$\boldsymbol{a_1} = \begin{bmatrix} \lambda + 2\mu & 0 \\ 0 & \mu \end{bmatrix}, \quad \boldsymbol{a_2} = \begin{bmatrix} \mu & 0 \\ 0 & \lambda + 2\mu \end{bmatrix}, \quad \boldsymbol{a_3} = \begin{bmatrix} 0 & \lambda + \mu \\ \lambda + \mu & 0 \end{bmatrix}. \tag{5.7}$$

Equation (5.6) defines the wave motion for an unbounded, linear elastic medium using the Lamé constants λ and μ. To complete the Lamb wave problem, Eq. (5.6) is supplemented by boundary conditions in the following section.

5.2.1.2 Boundary Conditions

Stress-free boundary conditions for Lamb wave propagation in 2-D space require that

$$\sigma_{ij}n_j = 0 \quad \text{at} \quad y = \pm h, \quad i = \{1, 2\}, \tag{5.8}$$

where $\boldsymbol{n} = \pm [0 \;\; 1]^T$ is the surface outward-pointing normal vector and $2h$ is the plate thickness. Equation (5.8) results in two sets of equations for the top, $y = +h$, and bottom, $y = -h$, surface

$$\pm \boldsymbol{b_1} \frac{\partial \boldsymbol{X}}{\partial x} \pm \boldsymbol{b_2} \frac{\partial \boldsymbol{X}}{\partial y} = 0, \quad \text{for} \;\; y = \pm h, \tag{5.9}$$

where $\boldsymbol{b_1}$ and $\boldsymbol{b_2}$ are

$$\boldsymbol{b_1} = \begin{bmatrix} 0 & \mu \\ \lambda & 0 \end{bmatrix}, \quad \boldsymbol{b_2} = \begin{bmatrix} \mu & 0 \\ 0 & \lambda + 2\mu \end{bmatrix}. \tag{5.10}$$

Equations (5.6) and (5.9) define the Lamb wave propagation problem for a plate in 2-D space.

5.2.1.3 Dispersion Relation

The Rayleigh-Lamb problem, given by Eqs. (5.6) and (5.9), assumes the solution of the form $e^{+i(kx + \omega t)}$ and results in (k, ω) pairs that define guided Lamb wave modes, i.e. the dispersion curves. Relating wavenumbers and frequencies—or, equivalently, wave velocities and frequencies—dispersion curves pertain to phase-frequency characteristics of elastic waves as both k and ω appear in the exponential phase factor. It needs to be pointed out that for the full picture of wave propagation characteristics, Eqs. (5.6) and (5.9) may be used to determine the amplitude-frequency, (α, ω), characteristics usually referred to as excitability curves (Kijanka et al. 2018).

The solution to the Rayleigh–Lamb problem cannot be carried out analytically and requires a numerical procedure. Most widely used are the method of potentials and the partial wave technique (Solie and Auld 1973). While the latter offers clear insight into the physics of the problem, it is most frequently used for practical analyses. Following this procedure (see (Packo et al. 2016) Appendix A), the solutions are given by

$$\boldsymbol{X} = \frac{1}{2} \alpha \left[u^{(S,A)} \quad v^{(S,A)} \right]^T e^{+i(kx + \omega t)} + c.c., \tag{5.11}$$

where $c.c.$ stands for the complex conjugate of all preceding terms and α denotes the wave amplitude. It clearly follows from the analysis that the modes display even or odd symmetry with respect to the plate's midplane, and are therefore called symmetric—$u^{(S)}$, $v^{(S)}$—and anti-symmetric—$u^{(A)}$, $v^{(A)}$—Lamb wave modes. Respective components $u^{(S,A)}$ and $v^{(S,A)}$ are given by

$$u^{(S)}: \quad \frac{k}{\gamma_L} cos\,(y\gamma_L) + \frac{2k\gamma_S}{k^2 - \gamma_S^2} \frac{sin\,(h\gamma_L)}{sin\,(h\gamma_S)} cos\,(y\gamma_S), \tag{5.12}$$

$$v^{(S)}: \quad i\ sin\,(y\gamma_L) + i\frac{2k^2}{k^2 - \gamma_S^2} \frac{sin\,(h\gamma_L)}{sin\,(h\gamma_S)} sin\,(y\gamma_S) \tag{5.13}$$

and

$$u^{(A)}: \quad i\,\frac{k}{\gamma_L} sin\,(y\gamma_L) + i\,\frac{2k\gamma_S}{k^2 - \gamma_S^2} \frac{cos\,(h\gamma_L)}{cos\,(h\gamma_S)} sin\,(y\gamma_S), \tag{5.14}$$

$$v^{(A)}: \quad cos\,(y\gamma_L) + \frac{2k^2}{k^2 - \gamma_S^2} \frac{cos\,(h\gamma_L)}{cos\,(h\gamma_S)} cos\,(y\gamma_S) \tag{5.15}$$

for symmetric and antisymmetric modes, respectively.

By employing the partial wave technique, the solution pairs, (k, ω), are found in two steps. First, partial waves (i.e. waves in infinite medium) are obtained from an eigenvalue problem obtained by combining (5.11) and (5.6). Second, combinations of partial waves that satisfy the boundary conditions, Eq. (5.9), are retained.

Figure 5.1 shows example solutions for a Rayleigh-Lamb problem for an aluminium plate ($\lambda = 60{,}500$ MPa, $\mu = 25{,}900$ MPa and $\rho = 2700$ kg/m^3), namely multi-modal dispersion curves in (k, ω) (Fig. 5.1a) and (V, ω) (Fig. 5.1b) spaces, and the corresponding excitability curves (Fig. 5.1c). Respective modes are labeled by a letter (S—for symmetric and A—for antisymmetric) and a subscript denoting the mode order. The fundamental antisymmetric and symmetric modes, A_0 and S_0 respectively, are most frequently employed for damage detection. Clear dispersive behaviour—i.e. frequency-dependent velocity—can be observed for all modes.

While interacting with defects, guided waves may undergo partial reflection, refraction, scattering and mode conversion. It means that the energy of the signal can be partially reflected back to the transmitter and convert to a different type of mode. Moreover, in the base of composite inspection, anisotropy plays a significant role, leading to directional dependence of wave velocity for each mode. Those characteristic features of guided waves are usually exploited in the detection of various defects such as cracks (Masserey and Fromme 2015; Chen et al. 2019; Mardanshahi et al. 2020; Barski and Stawiarski 2018), delaminations (Zhao et al. 2019; Munian et al. 2020; Raišutis et al. 2010) and bonding integrity (Yu et al. 2017; Ochôa et al. 2019; Vanniamparambil et al. 2015; Fan et al. 2013).

Despite that guided waves offer significant advantages over the conventional bulk wave testing, many limitations of their use in the majority of engineering structures are still present to overcome. Since many guided wave modes co-exist simultaneously, each having frequency and direction-dependent velocity, after several reflections and mode conversions the receivers usually capture overlapped and distorted time-domain signals that are difficult to interpret. The responses that are captured from defects are usually weak and may be concealed anywhere in the

received signal. Such a response captured from the structure varies from one geometry to another and depends on the type of excitation and environmental conditions, such as temperature, loads and movement-induced vibrations (Su and Ye 2006). In order to obtain useful measurement data it's necessary to excite and receive single guided wave mode minimising the coherent noise from other propagating modes. The variety of structures present in the aerospace sector, ranging from wing panels, to stiffened joints each time requires new developments in sensing, measurement and data analysis technologies. Hence, a deep understanding of the mechanism of guided wave propagation, spatial coverage, interaction with medium and the defects of interest is required for successful in-situ guided wave application.

5.2.2 Active and Passive Guided Wave Inspection

In general, guided wave inspection can be categorized into either active or passive. Passive techniques aim to record structural response induced by natural loads of the structure which happen during the flight of an aircraft. A comprehensive review of passive acoustic NDT techniques is presented in Chap. 7 of this book. One other good example of the passive technique is an embedded optical fibre Bragg grating sensor which has a series of parallel engraved lines (index points of refraction) that provide different reflection and transmission of light under varying strains in the structure. In case of fibre breakage, loss of transmitted light is observed, while the strain changes leads to altered refraction coefficient (Papantoniou et al. 2011). Optical fibre sensors have been extensively used to measure the temperature and strain of aircraft structures and even to detect the delamination type defects by analysing the wavelength shifts and reflection spectra of light (Ecke 2000; Takeda et al. 2002). Such inspection techniques are covered in Chap. 8. Active SHM utilizes both actuators and sensors to measure a response of the structure to a known input. Both bulk wave and guided wave techniques can be categorized as active, however in aerospace SHM applications the guided waves inspections are more commonly used. Guided wave excitation is usually determined by the design of the structural health monitoring system. It essentially depends on the type of defects which has to be detected and the structure under analysis. In the ideal case, the best guided wave mode for inspection should feature low dispersion and attenuation, high sensitivity to damage, easy excitability and detectability (Su and Ye 2006). The dispersion and attenuation depend on the excitation frequency and material properties, while the sensitivity to the defect is determined by the displacement profile of each mode.

5.2.3 Dispersion and Attenuation

High dispersion usually limits the sensitivity to the defect and the inspection length, as the wave-packet of the mode becomes distorted with the distance. To reduce the

effect of dispersion, narrowband excitation is usually applied by increasing the number of cycles of the excitation signal. As a result, the bandwidth of the signal decreases, limiting the extent of dispersion (Wilcox et al. 2001b). On the other hand, it means that the signal itself becomes longer in duration which reduces the temporal resolution. Wilcox et al. introduced a concept of minimum resolvable distance (MRD), which shows the sweet spot on the dispersion curve, where the best compromise between propagation distance, number of excitation signal cycles, wavelength and resolution can be estimated (Wilcox et al. 2001a):

$$\mathrm{MRD} = \frac{c_0}{d}\left[l\left(\frac{1}{c_{\min}} - \frac{1}{c_{\max}}\right) + T_{\mathrm{in}}\right]_{\min}, \tag{5.16}$$

where l and d are the wave propagation distance and the plate thickness; $c_{\min}$, $c_{\max}$ are the minimum and maximum velocities through the distance l; c_0 is the velocity at the central frequency; T_{in} is the initial time duration of the wave-packet. Typically, fundamental modes of guided waves such as A_0 and S_0 possess low MRD values and therefore require less cycles for adequate resolution.

Different post-processing strategies exist that can be used to reduce the effect of dispersion after the signal arrives to the sensor. For example, Wilcox presented a technique that uses a priori knowledge of dispersive characteristics of guided wave mode to compress the signals by mapping the time to distance domains (Wilcox 2003). De Marchi et al. introduced the warped frequency transform method to reduce the effect of dispersion. The authors used chirped pulse excitation with the proposed dispersion compensation technique to improve arrival time estimation in the detection of simulated defects on aluminium plate (De Marchi et al. 2013). However, in most cases the reconstructed signals are either still deformed due to non-linearity of the transformation function or the compensation methods are usually efficient for the reconstruction of one targeted mode (Luo et al. 2016). Recently, the sparse decomposition methods, that use a dictionary of non-dispersive signals to decompose guided wave responses obtained from the structures were proposed (Xu et al. 2018). The dictionaries are built exploiting the dispersion curves of the signal, which requires precise knowledge of the material properties. Each atom in the dictionary represents a dispersive signal at a certain distance. By comparing each atom to the measured signal, the non-dispersive analogue can be found.

Attenuation is another limiting factor that can influence the design of the monitoring system. Considering that the reflection from damage is usually weak, the attenuation of guided waves has to be sufficiently low in order to capture such reflections at some distance. The main factors that determine the level of attenuation are dispersion, beam divergence, material damping and leakage of the acoustic energy into the surrounding media (Long et al. 2003; Mustapha and Ye 2014). The leakage depends on the difference between the phase velocity of guided waves in the structure and the velocity of bulk waves in the surrounding medium. Significant leakage is observed in those cases when the phase velocity of guided waves is above the bulk wave velocity in the embedded media. The leaky behaviour of guided

waves are usually exploited while investigating flow and defects in gas or fluid loaded pipes (Djili et al. 2013; Zichuan et al. 2018; Mazzotti et al. 2014).

5.2.4 Guided Wave Excitation and Mode Selection

Ultrasonic guided waves can be excited using different strategies, depending on the application of the monitoring system. Direct contact methods can be either surface mounted or embedded into the structure. Surface-mounted sensors, like piezoelectric wafers are cheap, lightweight, can be arranged in different configurations and easily replaced if necessary (Giurgiutiu 2015). Simple instrumentation is required for such sensors as they operate on the direct and inverse piezoelectric effect. However, surface mounted solutions are not very attractive for in-situ applications as they change the aerodynamics of the structure. Thus for in-service aerospace monitoring systems, integrated sensors are preferred. These have high requirements for durability, as the monitoring system has to be reliable for the whole life-time of an aircraft. Different studies are available that analyse the durability of integrated sensors under varying environmental and cyclic conditions (Giurgiutiu et al. 2004; Melnykowycz et al. 2006; Tsoi and Rajic 2008). Different type of integrated sensors exists, while most commonly piezoelectric and fibre Bragg grating are used. Sensor integration can introduce additional resin-rich regions in the laminate or the sources of crack initiation around the corners of the piezoelectric sensor, therefore the shape and integration design has to be considered carefully taking into account overall strength of the host structure (Veidt and Liew 2012). Fibre Bragg grating sensors are lightweight and designed to be integrated into the composite structures. Such sensors do not require wiring, are cheap, durable and do not change the strength of the host structure (Veidt and Liew 2012; Majumder et al. 2008). Non-contact inspection methods like air-coupled or laser ultrasonics provide an ability to adjust to the complex surface of the structure. Such methods can be adjusted to excite different guided wave modes as the angle between the transducer and the sample can be easily adjusted (Panda et al. 2018; Römmeler et al. 2020). Laser and conventional air-coupled monitoring are usually combined, using conventional piezoelectric transducers for transmission and laser vibrometer for the reception (Jurek et al. 2018). Other researchers combined air-coupled ultrasonic testing with thermal imaging (Rheinfurth et al. 2011). Despite the advantages of air-coupled ultrasonic inspection, it requires some expensive equipment, such as scanners, laser heads etc. and also access to inspected parts; hence, it can be performed only during the maintenance break of an aircraft.

In real-world situations, using many abovementioned guided wave excitation methods multiple modes are being generated simultaneously, unless some specific excitation strategies are applied. Many studies are available that seek to excite specific mode of guided waves (Lee et al. 2008; Li et al. 2016). The simplest solution is to select specific operating points of guided wave dispersion curves, where only a desired modes exist. For example, at low frequency-thickness products, fundamental

zone with zeroth order modes exist. Such modes possess relatively simple mode shapes, are less dispersive and may be easily generated. Limiting the excitation bandwith and operating at low frequencies can effectively control number of modes present in the structure and the amount of their dispersion. At very high frequency-thickness products (20 MHz · mm and above), higher order guided wave modes have similar group velocities, hence they form a non-dispersive cluster which is called Higher Order Mode Cluster (HOMC) (Jayaraman et al. 2009). Such cluster of modes possess reduced surface sensitivy, thus it's a good choice for localised flaw detection, like pitting corrosion. In the medium frequency-thickness range, many modes exist which are usually dispersive and possess much more complex mode shapes. Inspection at such operating point provides better sensitivity to small defects and thickness variations which is achieved at a cost of mode purity. In order to supress unwanted modes, some of the following techniques could be mentioned. For instance, in case of air-coupled or laser beam excitation, the ultrasonic signal can be introduced at some incidence angle, which allows to excite specific modes and reduce coherent noise. Such incidence angle is frequency-dependent and may be calculated analytically. This selective mode excitation approach is usually valid for fundamental modes only, as the incident angles of different modes tend to overlap at higher frequencies.

In case of direct sensor placement on the surface of component, different selective mode excitation strategies must be applied. Giurgiutiu et al. used piezoelectric wafer active sensors to excite single guided wave mode (Giurgiutiu 2005; Xu and Giurgiutiu 2007). For a particular mode, the maximum of the strain and displacement functions is achieved when the width of the transducer is equal to odd multiple half wavelengths of the desired mode. In contrast, the minimum occurs in case the width of the sensor is equal to an even number of half wavelengths. In such a way, the size of the transducer introduces spatial filtering phenomena, which allow to enhance or suppress the vibrations of the particular guided wave mode (Giurgiutiu 2011; Samaitis and Mažeika 2017). Another approach for excitation of single guided wave mode is based on the use of interdigital or comb transducers, which consist of two-finger type electrodes that are interchanged and driven by an opposite phase electrical field (Monkhouse et al. 2000; Bellan et al. 2005). The type of mode which is introduced to the structure is determined by the pitch between finger electrodes which has to be equal to half the wavelength of the desired mode. Several design extensions of the classical interdigital transducers can be found, which were proposed by Salas et al. (Salas and Cesnik 2009) and Jin et al. (Jin et al. 2005). Glushkov et al. used a co-axial ring-type transducer for selective omnidirectional mode excitation (Glushkov et al. 2010). The major drawback of piezoelectric wafers and interdigital transducers is that the mode selectivity is related to the size of the transducer. It means that the set of sensors is required to excite different modes. At low frequencies, the physical dimensions of such transducers become large and not convenient for many applications.

Other approaches to generate a single mode are based on the positioning of two or more piezoelectric elements in a sequence on the surface of the sample at the inter-element distance equal to the wavelength of the desired mode (Grondel et al. 2002).

Similarly, elements can be positioned on the opposite surfaces and in-phase or out-of-phase excitation is then used to drive the mode of interest (Seung and Hoon 2007). The use of the phased-arrays is another field that contributes to the selective guided wave excitation. Fromme used 32-element circular array and phase addition algorithm to excite A_0 mode on aluminium plate (Fromme et al. 2006). The abovementioned approaches are most suitable for excitation of fundamental guided wave modes such as A_0 or S_0. It has to be considered that all modes of the wavelength determined by the pitch of array elements will be excited, which is especially important working with higher-order guided wave modes, thus reducing the mode selectivity. To overcome such a problem, recently Veit et al. proposed an approach for selective guided wave excitation using conventional phased array probe having small pitch relative to wavelength of targeted mode. By controlling the input signal bandwidth and the angle of generated beam even higher order modes can be excited both on metallic and composite structures (Veit and Bélanger 2020).

Different researches show, that the mode purity is an important issue for selective guided wave excitation. Usually, the approaches described above can produce some dominant modes; however, other modes might exist with significantly lower displacements and contribute to an overall noise of the signal. Other transducers, especially phased arrays, possess low dynamic range, thus they are limited to detection of relatively large defects.

5.3 Defect Detection

Guided wave defect detection methods can be categorized into baseline and baseline-free. The baseline methods require a baseline dataset, which describes defect-free state of the structure. Then each further collected signal is compared to a baseline to detect the presence of damage. If there are any structural changes present, the guided waves will be reflected or scattered by them. Subtracting such signal from baseline will give the residual, which may indicate the presence of damage. This technique allows to eliminate permanent reflections from object boundaries. Despite it's simplicity, such technique is extremely sensitive to changes of surrounding temperature, loads, transducer bonding, aging etc. For instance, some investigations show, that if magnitude of the reflection from the defect is at least –30 dB compared to the direct arrival, the temperature change of 10 °C can conceal the defect even though temperature compensation techniques are used (Croxford et al. 2010; Dai and He 2014). In order to make baseline subtraction work, non-damage related patterns have to be eliminated. The strategies to rule out the temperature influence on guided wave signals are discussed in more details in the POD section of this chapter.

The baseline free methods do not require a set of baseline signals, thus are less susceptible to envinronmental changes, transducer bonding, etc. Time reversal techniques can be presented as an example of baseline free damage detection (Sohn et al. 2007). Such approach uses at least two transducers where one of them

is dedicated for time reversal of the signal received from the first sensor and reemits it back. The whole procedure can be described as follows:

1. the wave is introduced into the structure by applying the voltage $V_A(t)$ to transmitter A;
2. the propagated wave is captured by sensor B and recorded as voltage $V_B(t)$;
3. signal $V_B(t)$ is reversed in time and reemitted back to transducer A;
4. finally, transducer A receives the signal $V_{BA}(t)$ and compares it with the original input $V_A(t)$.

For a defect-free structures, the input signal $V_A(t)$ should correlate to the reconstructed signal $V_{BA}(t)$, while any mismatch indicates structural changes (Park et al. 2009; Mustapha and Ye 2015). Some studies show that such a technique is not suitable for notch detection in metallic structures, as such defect does not break the time reversibility and only changes the amplitude of the received signals (Gangadharan et al. 2009). It should be also noted during analysis that the reciprocity of the system is only limited to the directly arriving waves. Boundary reflections and non-uniform distribution of attenuation properties may cause asymmetry in wave fields and differences between the original and the re-sent time-reversed signals, especially for multi-modal wavefields.

5.3.1 *Defect Localisation and Imaging: Sparse, Phased Arrays and Guided Wave Tomography*

Both abovementioned methods are dedicated to detecting structural changes. Unfortunately, these are not suitable to localize and characterize damage. In general, two defect detection approaches based on sensor type and placement can be identified—sensor networks or sparsed arrays and phased arrays (Rocha et al. 2013; Michaels 2016). Sparse arrays use a distributed network of discrete omnidirectional transducers which are positioned at specific regions of interest. Meanwhile phased arrays use closely spaced elements and are based on steering of the wavefront at different directions by applying different lag to each array element. Despite different sensor architectures, all damage detection and localisation methods are based on the assumption that any present discontinuity will produce an unexpected echo, which can be received by sensor.

Defect localization methods are mostly based on time-of-flight (ToF) measurement of defect scattered guided wave signals. In the simplest 1D case damage can be localized as shown in Fig. 5.2a. In such arrangement, the distance l_0 and signal arrival time T_0 between sensors A and B are known. In case of the defect, an additional reflection will be received by sensor B at time instant T_1. The distance x to the defect can be calculated according to the equation (Dai and He 2014):

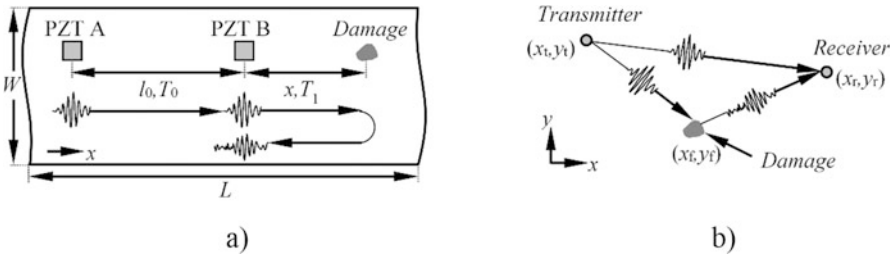

Fig. 5.2 The concept of damage localization in 1D (**a**) and 2-D (**b**) case (Dai and He 2014; Michaels and Michaels 2006)

$$\frac{l_0}{T_0} = \frac{2x}{T_1}. \tag{5.17}$$

This works well in presence of single mode only, however the corrections are necessary in case of mode-conversion. In 2-D case (Fig. 5.2b), the spatial defect position can be estimated by calculating the ToF of the signal going from the transmitter through the flaw (Michaels and Michaels 2007):

$$t_{\mathrm{tr}}^{\mathrm{f}} = \frac{\sqrt{(x_{\mathrm{t}} - x_{\mathrm{f}})^2 + (y_{\mathrm{t}} - y_{\mathrm{f}})^2} + \sqrt{(x_{\mathrm{r}} - x_{\mathrm{f}})^2 + (y_{\mathrm{r}} - y_{\mathrm{f}})^2}}{c_{\mathrm{g}}}. \tag{5.18}$$

where subscripts *t*, *r*, and *f* denote the 2-D coordinates of the transmitter, receiver and flaw. To detect damage location with sparsed array, at least three sensors are required. By using triangulation method it's possible to find an intersection of three regions produced by the sensors, where the possible damage is likely to occur. The shape of regions of the likely defect position will depend on transmission and reception approach. If the measurements are taken recording an echo received by each transducer and the wave propagates spherically, the region of the sensor will be in the shape of circle. On the other hand if each transducer acts as transmitter once, while all the transducers act as receivers, the region of the sensor will be in the shape of ellipse (Rocha et al. 2013). Such approach works well if wave velocity is the same in every direction. Otherwise the corrections have to be made and the actual location of the damage will be different. By using at least three sensors the image over the region of interest can be generated. In case of N sensors, the defect scattered signals will arrive at different time instances for each transmitter-receiver pair, depending on actual defect position leading to $N(N-1)/2$ different signals paths. To create an image, the evenly spaced grid points over the inspection area are defined. Then the pixel value at the reconstruction point (x,y) according to the delay and sum (DAS) algorithm can be estimated as (Michaels 2008):

$$P(x,y) = \frac{1}{N}\sum_{n=1}^{N}\left|\omega_{nxy} r_n\left(t - t_{nxy}\right)\right|^2 \tag{5.19}$$

where ω_{nxy}—is reconstruction weight at specific point (x,y), t_{nxy}—is the time delay which can be calculated as d_{nxy}/c_g where d_{nxy}—distance from transmitter through point (x,y) to receiver, c_g is the group velocity. Then the 2-D defect map can be created, by repeating this procedure at spatially distributed reconstruction points. At the actual defect locations, such addition will lead to constructive interference of received signals. The major drawback of the DAS method is a large point spread function and artefacts which may be caused by wave reflections from the boundaries and mode-conversion (Michaels 2016).

Reconstruction algorithm for probabilistic inspection of defects (RAPID) method can be shown as another example of sparse array imaging (Zhao et al. 2007). RAPID method uses a circular arrangement of the sensors and assumes that most significant signal changes appear in the direct wave path. Hence, between each transmitter receiver pair a linearly decreasing elliptical spatial distribution of signal change effects due to defects is presumed. In case of N PZT elements, the defect probability at imaging position (x,y) can be expressed as (Zhao et al. 2007):

$$P(x,y) = \sum_{i=1}^{N-1}\sum_{j=i+1}^{N} P_{i,j}(x,y) = \sum_{i=1}^{N-1}\sum_{j=i+1}^{N} A_{i,j}\left(\frac{\beta - R_{i,j}(x,y)}{\beta - 1}\right), \tag{5.20}$$

where $P_{i,j}(x,y)$ is defect distribution probability estimate for i^{th} transmitter and j^{th} receiver, $A_{i,j}$ is signal difference coefficient of the same sensor pair, $(\beta\text{-}R_{i,j}(x,y))/(\beta\text{-}1)$ is the lineary decreasing elliptical spatial distribution. Different indicators can be used for 2-D reconstruction of the defect position and definition of the pixel value in the reconstruction grid using sparse arrays. For example, Kudela et al. (Kudela et al. 2008) used a concept of damage influence map, which measures the match between the excitation signal and reflection from defect. The idea is based on the arbitrary positioning of the excitation signal on the response from the structure employing different time delays. The delay applied to the signal is then equal to the ToF from the transmitter to the likely damage position. The match between two signals at location (x,y) here is expressed by (Kudela et al. 2008):

$$e_k(x,y) = \int_{t_0}^{t_0+\Delta t^*} \widehat{S}_T(t)\left[F(t)G\left(x,y\right)\widehat{S}_{R,k}(t)\right]dt, \tag{5.21}$$

where t_0 and Δt^* are the start and the width of the time window; $\widehat{s}_T(t) = S_T(t_0, t_0 + \Delta t*)$ is the windowed excitation signal; $\widehat{S}_{R,k}(t) = S_{R,k}(t_0 + \Delta t, t_0 + \Delta t*)$ is the signal registered with the k^{th} receiver, $F(t)$ is the window function (Gauss, Hann, etc.); $G(x,y) = e^{\alpha(d0P+d\text{Pk})}$ is the function dependent on the attenuation; α is the attenuation coefficient; d_{0P} and d_{Pk} represent the distances

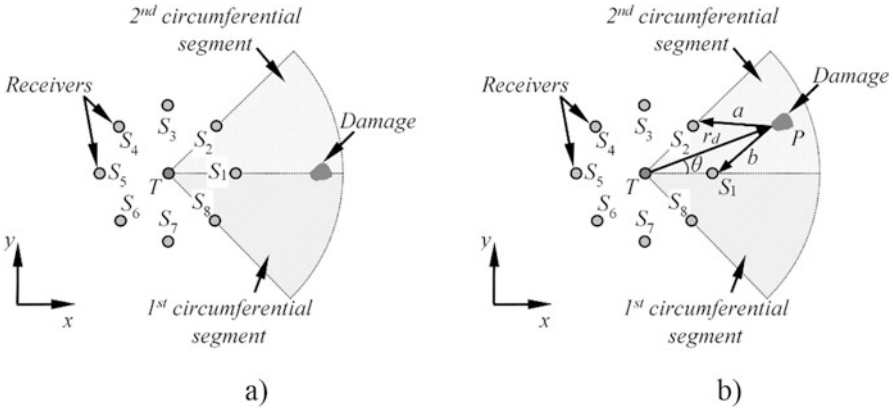

Fig. 5.3 The concept to determine the radial segment of the damage location (**a**) and the idea of exact damage positioning using the triangulation method (**b**) (Giridhara et al. 2010)

between the transmitter-imaging point and imaging point-receiver; Δt is the signal time shift, which depends on the x, y coordinates of the imaging point and the group velocities c_{0P} and c_{Pk}. The total match at location (x,y) for all transmitter-receiver pairs can be expressed as (Kudela et al. 2008):

$$E = \sum_k \int_S e_k(x,y)dS \approx \sum_k \sum_{i,j} e_k(x_i, y_j), \tag{5.22}$$

Modifications of the proposed technique exist, which were introduced by Wandowski et al. (Wandowski et al. 2011; Wandowski et al. 2016). A slightly different approach was used by Michaels (Michaels and Michaels 2007), where authors used band pass filters with various central frequencies to obtain a set of bandlimited signals for each transmitter-receiver pair. Then the defect map is being created for each central frequency of the applied filter. Eventually, all individual images are combined taking minimum pixel value from all corresponding images, which minimizes phasing and other artefacts.

A modification of sparse array architecture was proposed by Giridhara et al. (Giridhara et al. 2010) who implemented the radial segmentation technique. It consists of a single transmitter and radially distributed receivers, which divide the object into circumferential segments. The signals from neighbouring transducers are compared to determine the location of the defect. If the flaw is somewhere along x axis (Fig. 5.3a), the sensor signals (S_2 and S_8; S_2 and S_1; S_1 and S_8) will indicate some changes in the structure. If two signals from sensors S_2 and S_8 match, then the damage is in the segment S_1 and S_2 or in the segment S_1 and S_8. The radial segment of the defect is determined by measuring the ToF of the reflection from the flaw with sensors S_2 and S_8. The exact defect angular, θ, and radial, r_d, position estimates are found by using triangulation as shown in Fig. 5.3b (Giridhara et al. 2010):

$$\theta = \phi + \cos^{-1}K; \phi = \tan^{-1}\left(\frac{py_{i+1} - qy_i}{px_{i+1} - qx_i}\right); K = \cos(\theta - \phi). \tag{5.23}$$

$$r_d = \frac{p}{2(x_i \cos\theta + y_i \sin\theta - d_i)} = \frac{q}{2\left(x_{i+1} \cos\theta + y_{i+1} \sin\theta - d_{i+1}\right)}, \tag{5.24}$$

where $p = x_i^2 + y_i^2 + d_i^2, q = x_{i+1}^2 + y_{i+1}^2 + d_{i+1}^2$, d_i and d_{i+1} are the total travel path from the transmitter through the flaw to the sensors S_i and S_{i+1} respectively ($d_i = r_d + a$, $d_{i+1} = r_d + b$, $r_d = x^2 + y^2$); a and b are the distances of the sensors $S_i(x_i,y_i)$, S_{i+1} (x_{i+1},y_{i+1}) to the damage P ($a^2 = (x–x_i)^2 + (y–y_i)^2$, $b^2 = (x–x_{i+1})^2 + (y–y_{i+1})^2$).

The sparse array approach interrogates the damage from multiple angles, hence the forward scattered and backscattered signals can be recorded if the damage is present within the area of array. Moreover, the reflection energy from the defect is more uniform within the region of sparse array in contrast to phased array inspections. On the other hand, as the phased array elements are located in close proximity to each other, it's much easier to leverage the phase difference which is mainly caused by errors in phase velocity, transducer locations and variation of transducer characteristics (Michaels 2016). Using the phased array imaging, the array elements are delayed so that the azimuth of the wave φ is equal to the azimuth of target reflector φ_0. To obtain the target direction most of phased array methods sweep the beam at different directions and estimate the maximum of received signal energy. Once the target direction φ_0 is obtained, the distance to the reflector can be estimated using cross correlation or other time delay measurement method. An example of phased array imaging can be embedded ultrasonic structural radar (EUSR) method (Giurgiutiu and Bao 2004; Purekar et al. 2004). The use of phased arrays offers some advantages over single transmitter-receiver measurements, such as steering and focusing, hence large area of the sample can be examined and direction of reflector can be determined almost instantly. However, in practice due to multiple reflections and structural noise it becomes difficult both to distinquish reflector and to measure the time-of-flight precisely, which leads to defect positioning errors. Aircraft components made from composite materials introduce additional complexity for damage detection and localisation. The mechanical properties of composites are direction dependent, hence the circular or elliptical damage regions are no longer valid. Phased array beam steering becomes more complex, as radial velocity distributions must be known. As the velocity of guided waves varies with the propagation direction, wavelength and operating point on the dispersion curve (and dispersion itself) change as well. It means that the sensitivity to the defect and resolution are changing, especially if operating point is located on the dispersive region of the selected mode. This shows that each unique structure requires adaptation of the monitoring system—determination of radial velocity distributions, evaluation of boundary reflections (taking into the account velocity information), identification of present modes. Guided wave tomography is one of the most common imaging methods used to detect and localize structural changes. The tomography aims to reconstruct the spatial distribution of the material properties, which can be based on the projection of wave velocity, attenuation, frequency shift or other features

(Belanger and Cawley 2009). To get the desired resolution, a large number of projections are required which can be collected either using transmission or reflection approach. Among the sensor arrangement topologies, the crosshole, double-crosshole and fan-beam are the most popular ones (Park et al. 2020). Several different tomographic reconstruction techniques exist, namely straight-ray, bent ray and diffraction tomography (Belanger and Cawley 2009; Willey et al. 2014; Belanger et al. 2010). The straight-ray methods neglect refraction and diffraction assuming that projection data corresponds to a line integral of given parameter. Bent ray methods take into account wave field of reflected from the defect, while diffraction tomography is based on Born's approximation.

5.3.2 Guided Wave Interaction with Actual Structural Defect

The damage detection and localisation principles described above exploit many assumptions that simplify the reconstruction. In realistic structures, the reponse of the defect is much more complex. For example, delamination is one of the most common defects found in multi-layered structures, which develop internally between neighbouring layers of the laminate. After the interaction with delamination, guided waves are scattered and convert to other modes (Feng et al. 2018). Various researches show that fundamental modes of guided waves propagate separately in two sub-laminates created by defect and then interact with each other after exiting the damaged area. A detailed guided wave interaction with delamination type defects was presented by Ramadas et al. who found that in case of delaminations positioned symmetrically across the thickness of the laminate, incident A_0 mode converts to S_0 within the defect and then back to A_0 after exiting. For asymmetrical defects, the mechanism is slightly different as an additional S_0 mode is present upon interaction with defect (Ramadas et al. 2009; Ramadas et al. 2010). It was also observed by various research groups that Lamb wave scattering at the beginning and tip of defect is determined by its position. Schaal et al. estimated frequency-dependent scattering coefficients for fundamental Lamb wave modes at both ends of the defect (Schaal et al. 2017). Based on this approach, Hu proposed a technique to locate delamination defects based on reflection and transmission coefficients of A_0 and S_0 modes (Hu et al. 2008). Shkerdin and Glorieux (Shkerdin and Glorieux 2004) related the transmission coefficients of Lamb waves with the depth and length of delamination, while Birt et al. (Birt 1998) analyzed the magnitude of reflected S_0 mode and its relation to the width of delamination. This shows that different indicators can be developed to detect defects and to assess their parameters. A complex guided wave scattering and mode conversion upon interaction with defects allows to develop various tools to identify and characterize the damage. In most simple cases, ToF measurements of reflected and transmitted guided wave modes can be used to detect the existence and location of the damage. Furthermore, by analysing the magnitude patterns and velocities of guided wave modes, other features like defect size and depth can be extracted.

5.4 Reliability of SHM Systems

SHM is a technique used for monitoring the integrity of in-service structures of aircraft, bridges, piplines and other components which are continuously exposed to operational load and environmental influence. The goal of SHM technology is to complement NDE techniques to improve reliability of the structure and reduce inspection and repair costs (Meeker et al. 2019; Etebu and Shafiee 2018). Thus, performance of the SHM system is characterized by the quality of sensors, their mounting and reliability of measurements. Reliability of SHM system depends on the quality of received data (Li et al. 2019; Datteo et al. 2018). SHM systems and NDE techniques use the same physical principle for damage detection. However, there are notable differences between the two systems. SHM measurements are carried out by the same array of sensors fixed in the same locations and provide continious monitoring of the structure. Hence, in contrast to traditional NDE, each new result obtained from sequentially repeated inspections depends on the previous one in SHM system. Assessment of structural integrity is characterized by a large period of time between the first and last inspection in sequence of NDE technique. Conversely, when short time period passed the process is called monitoring. Therefore, SHM is able to control structural integrity in real-time and detect damage before the scheduled maintenance. Another essential distinction of SHM and traditional NDE are the different causes which affect the measurements (Kabban et al. 2015). In the case of SHM application the sources of variability are not the same as for NDE. For instance, NDE variables as sensors, instrumentation and operator are fixed parameters in SHM. Sources of variability in SHM are mostly relate to in-situ effects, such as temperature, aging and load variation. Additionally, key point of SHM system is a fixed nature of sensing probes which leads to a lack of variation in sensor response caused by human factor. If the variability of in-situ effects is low or it can be filtered, the SHM registers variability of the system to defect geometry, inconsistencies of sensors mounting and structural differences (Fisher and Michaels 2009; Cobb et al. 2009).

In order to ensure reliability of SHM system the following activities have to be performed (Etebu and Shafiee 2018; Kabban et al. 2015):

1. Perfect communication between specialists who install sensors and specialists who carry out structural analysis;
2. Careful planning of areas to monitor;
3. Sensor system design;
4. Component replacement design;
5. Data storage design;
6. Testing of sensors system;
7. Aging compensation of sensors.

Reliability of SHM is the evaluation of probability of repeated and successful outcomes of the system under prescribed environmental conditions. Reliability

indicates the quality of fault detection by assessment of four probabilities (Stolz and Meisner 2020; Gallina et al. 2013):

1. Probability of detection (POD)—the system detects faults when they exist in the structure;
2. Probability of false alarms (PFA)—the system detects faults when they do not exist in the structure;
3. Positive predictive probability (PPP)—the system detects no faults when they exist in the structure;
4. Negative predictive probability (NPP)—the system detects no faults when they do not exist in the structure.

Since PPP and NPP are the inverse probabilities of POD and PFA, only first two probabilities have to be assessed. Great attention has to be paid to false calls because they occur often in SHM. POD and PFA are also interdependent through the threshold which defines the level of the system response indicating the presence of damage in the structure (Gallina et al. 2013).

5.4.1 Basic Concepts of POD and PFA

POD is the probability of specified NDE inspection to detect defects in the structure at the time of inspection. MIL-HDBK-1823A provides all statistical tools and procedures to assess POD for reliability validation of NDE techniques. Usually, POD is a function of defect characteristics, i.e. length of the defect. Log Odds and Log Probit probabilistic models are commonly used for POD assessment (Gallina et al. 2013; Aldrin et al. 2016). POD can be assessed by Hit/Miss and signal response analysis. The objective of both configurations is to produce a POD curve vs characteristic parameter of the defect (usually size). Typical POD curve is presented in Fig. 5.4.

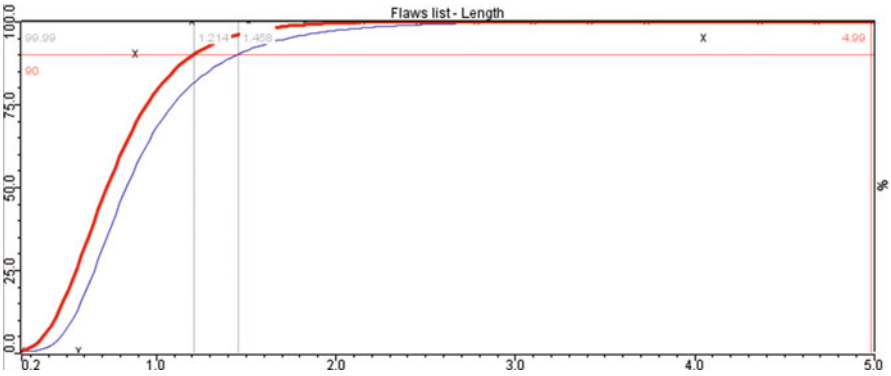

Fig. 5.4 Typical POD curve received by Hit/Miss analysis in red and POD with 95% confidence level in blue

Small size of the defect is characterized by 0 POD (0%) meaning that the system could not detect defect of the specified size. The POD is 1 (100%) in the case of large defects meaning that the system detects defect of specified size reliabily. Transition zone where POD curve is increasing between 0 and 1 is under most interest. Additionally, the confidence interval is associated with POD and indicates the content of true value in the interval (Chapuis et al. 2018a; Chapuis et al. 2018b). Hence, confidence bounds characterize the ability of the system to detect particular characteristic parameter (defect size) with defined probability and confidence (Gallina et al. 2013). The usual requirement, especially for aerospace applications, is to determine the minimum size of defect which is detectable in 90% of the inspections at 95 % confidence level, $a_{90/95}$ (Gallina et al. 2013).

Hit/Miss approach is characterized by measurement of qualitative information and determines the presence or absence of the damage. The response of the inspection is binary value of 1 (defect is detected) and 0 (fail to detect the defect). The model of POD in Log-Odds functional is expressed (Chapuis et al. 2018b):

$$\mathrm{POD}(a) = \left[1 + \exp\left(-\left(\frac{g(a) - \mu}{\sigma}\right)\right)\right]^{-1}, \tag{5.25}$$

where a is a characteristic parameter (defect size), $g(a) = a$ or $g(a) = \log(a)$, μ is a defect size detected with a probability of 50% and σ is the steepeness of the function.

Also, POD can be evaluated by signal response approach (â vs a) or quantitative measure of defect size. POD curve is based on methodology when there is a relationship between the defect size, a (physical dimension of a defect size), and sensor response â (measured response of the system to a target size). In the case of ultrasonic inspection the system provides a response from the defect whose amplitude is dependent on it's size. Signal response approach is able to estimate and build POD curve using greatly smaller amount of data comparing to Hit/Miss analysis (Meeker et al. 2019; Chapuis et al. 2018b). Generally, this approach has a linear model and is expressed as following (Chapuis et al. 2018b):

$$y = \beta_0 + \beta_1 g(\mathrm{a}) + \varepsilon, \tag{5.26}$$

where β_0 and β_1 are the coefficients of linear function, $g(a) = a$ or $g(a) = \log(a)$, ε is a random error.

Since the noise exists in any inspection data the boundary which determines damage or no damage output has to be established. For this task the the detection threshold a_{thres} is fixed. Further, the POD curve can be expressed as a function of density of scattered data which is above the detection threshold y_{thres} (Gallina et al. 2013; Chapuis et al. 2018b):

$$\mathrm{POD}(a) = \mathrm{P}(y > y_{\mathrm{thres}}) = 1 - \Phi_{norm}\left(\frac{y_{\mathrm{thres}} - (\beta_0 + \beta_1 g(a))}{\sigma_\varepsilon}\right)$$
$$= \Phi_{norm}\left(\frac{g(a) - \mu}{\sigma}\right), \tag{5.27}$$

where $\Phi_{norm}(z)$ is the normal density function and $\mu = \frac{y_{\mathrm{thres}} - \beta_0}{\beta_1}$, $\sigma = \frac{\sigma_\varepsilon}{\beta_1}$. The parameters μ and σ are determined according to the methodology of maximum likelihood estimation (Chapuis et al. 2018b).

As it was mentioned in Sect. 5.4, the probability of false alarms or Relative Operating Characteristics (ROC) curve has a significant importance to estimate the performance of SHM and NDE systems (Gallina et al. 2013). Selection of adequate detection threshold is an essential part in PFA assessment. It is a high possibility to classify undamaged regions of the component as damaged due to high number of observations in SHM system. For instance, the detection threshold can be exceeded by the impact of strong background noise when no defect is present. However, the POD and PFA are spatially dependent. Therefore, in order to determine appropriate detection threshold it is useful to plot POD and PFA in the same diagram to establish the overlap between two metrics of system performance (Fig. 5.5) (Gallina et al. 2013; Chapuis et al. 2018b; Schoefs et al. 2012).

In the case of NDE inspections a_{thres} is determined from the measurement when no flaw in the structure is present and the value is set above the background noise level. Since the threshold is set quite high in NDT applications the PFA has usually a low value (Fisher and Michaels 2009). Consequently, the threshold value in NDE for signal response approach is the highest level of noise in the defect free region (Fisher and Michaels 2009). However, it is a challenging task to determine detection threshold for SHM application. In the case of SHM system, a number of measurements of not defective structure will be available before damage occurs. Since the sensors are fixed in SHM system, in-situ effects will affect the signal response—temperature, operational load or sensor degradation. As a result, detection threshold can be determined as a variance in signal response over time from the undamaged structure. Another complexity to define a_{thres} is a dependent measurement of SHM. Due to a large degree of variability the measurement response can be classified as damage even if there is none in accordance with prior measurements (Meeker et al. 2019; Fisher and Michaels 2009; Cobb et al. 2009).

5.4.2 Sources of Variability of SHM System

Before POD assessment , NDE and SHM systems should be completely evaluated in terms of the limits of operational parameters and application in order to list factors that significantly affect the variability of the system (Department of Defense 2009). It is essential to capture all sources of variability. Otherwise, the results of system performance evaluation will be invalid due to missed significant variables. After

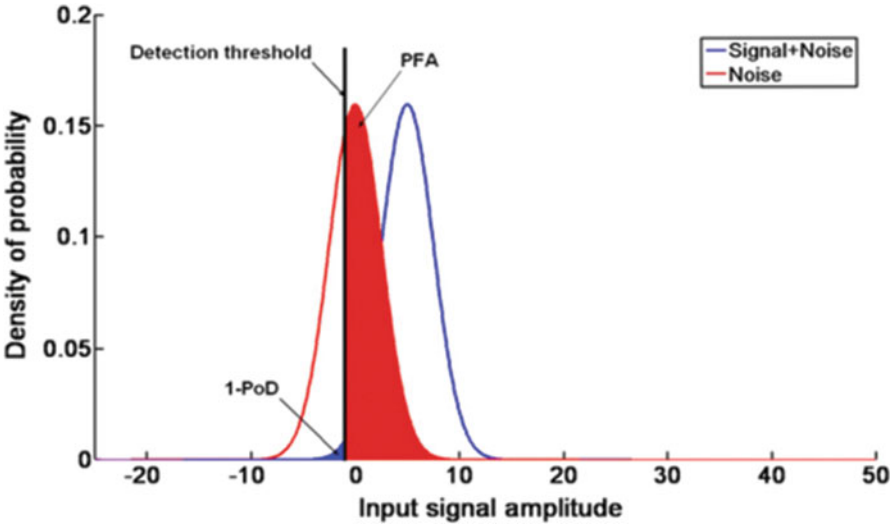

Fig. 5.5 Plot of POD and PFA (Schoefs et al. 2012)

analysis, variables which have negligible impact on the detection can be eliminated (Mandache et al. 2011). There is a risk to overestimate the POD of smaller size defects and underestimate the PFA in the case of missing important influential sources. Factors of SHM system which could affect the signal are as follows (Meeker et al. 2019; Mandache et al. 2011):

1. Shape, size and orientation of the defect as well as the change of these characteristics over time;
2. Defect and sensor location;
3. Environmental conditions (temperature, humidity);
4. Mechanical variables;
5. Change of structural configuration over time;
6. Change of sensor performance over time;
7. Quality of sensor bonding;
8. Sensor degradation and aging;
9. Ambient noise;
10. Dirt;
11. Electromagnetic radiation;
12. Mechanical loads;
13. Data communication.

One of the advantages of SHM system is a reduction of human intervention as an important factor affecting the results due to automatization. However, there is still human involvement in the case of instrumentation installation and interpretation of the recorded data if required, but manual coordination is avoided (Mandache et al. 2011).

To ensure reliable work of SHM system backup power provision has to be implemented, since, power line is often at the risk to fail during emergency cases. Furthermore, SHM sensors durability depends on the power requirements. In the case of battery power supply, low weight and charging capabilities has to be feasible. More appropriate solution is to use self-powered sensors through energy harvesting. Additionally, to reduce the problem of sensors failure within years of exploitation they have to be self-diagnosed or redundant. Redundant SHM system involves sensors, which are not expensive and easy to install. The approach essence is to install multiple number of sensors with overlapping range to provide redundant sensing. Consequently, if one of the sensors fails, the others take over and perform the task. This redundant configuration can create more defect-tolerant and robust system (Mandache et al. 2011; Aldrin et al. 2013). However, redundant elements increase the weight of the system, which, especially in aerospace, should be kept as low as possible.

The sensors have to be optimally placed to assure the sensitivity to the damage as well as condition of structure surface. The guided waves have the ability to confine in thin-wall structures, so they are able to propagate over large distance of the structure with minimal loss of energy and attenuation. In addition, the guided waves are suitable for the inspection of various shapes and geometries of the long structures. Therefore, it is possible to monitor the condition of surface of the structure of different shape. Generally, the more sensors are placed on structure the more detailed information about structure health is received. The coverage of the sensors should be performed in specific way in order to provide adequate information from collected data. Performance requirement and sensor network robustness have to be fulfilled (Mandache et al. 2011; Yi and Li 2012; Abbas and Shafiee 2018).

In the case of monitoring high risk zones the sensors should be placed in close proximity in order to have higher sensitivity in the case of damage occurrence but not placed in potential risk of impact damage place since this can affect the sensor itself (Mandache et al. 2011).

A good quality of coupling between sensor and structure has to be provided. Usually, adhesive is used as a coupling medium. However, degradation of adhesive properties can also affect on the response of the sensor. In aerospace industry during aircraft exploitation, sensors which are placed on the surface of the structure are not applicable due to aerodynamic conditions. This method is possible on the measuring stands in laboratory conditions (Mandache et al. 2011).

Traditional wired SHM system consists of sensor system, data communication and storage system as well as the information analysis system to assess the integrity of the structure. The main disadvantages of wired system is a high cost of long cables, low productivity, time consumption, low flexibility, impact on the weight of the structure and heavy traffic of monitoring channels (Wang et al. 2020). Wired system is exposed to cable and wire breakage during the exploitation and leading to system malfunction. Wireless sensor networks have advantages of low cost, high efficiency, high flexibility. There are various protocols of communication technology widely described in (Alonso et al. 2018). Selection of the communication technology is dependent on the characteristics of infrastructure and monitoring

requirements. However, if the data is transmitted and stored wirelessly there is still issues on the effect of SHM system interaction with other aircraft systems and avionics, electromagnetic and radio frequency interferences, what data has to be collected and at what frequency and etc. (Mandache et al. 2011).

5.4.3 Analysis of Environmental and Operational Conditions

In order to define methodology for verifying reliability of SHM it is necessary to understand how sensors and other factors respond to the damage. In the case of guided waves, environmental and operational conditions can change the phase and the amplitude of the signal. The challenge in SHM system is to identify signal changes due to the damage presence from the false calls caused by the environmental and operational parameters influence. Guided wave technique is a suitable tool for damage detection and characterization, however, it has a high sensitivity to these factors. According to the work performed in this field, the impact of these parameters is compensated by development of appropriate modelling process, variation of sensor technologies, processing of the acquired signals, extraction of features as well as statistical methods and machine learning (Mandache et al. 2011; Gorgin et al. 2020). Environmental and operational conditions are huge source of variability in aerospace industry, civil and mechanical engineering. In this section, temperature and mechanical loading are discussed more widely due to their significant influence on SHM systems.

Temperature is the important condition, variation of which is limiting the guided wave SHM systems. Temperature change is dominant influential property of environment condition that affects robustness of guided wave SHM (GWSHM) system (Fendzi et al. 2016). Temperature affects the component under monitoring and the sensing system. Propagation characteristics of Lamb waves significantly depends on temperature variation. Volume and density of the component changes with the temperature variation. This leads to a modification in the elastic properties, change of ultrasound velocity in the material that influence the response of the sensor at damage free place in the component (Mandache et al. 2011).

In order to mitigate this problem many investigations on the change in guided waves properties caused by temperature were conducted experimentally, numerically and analytically. Different configurations of the technique as well as temperature range was studied. Generally, by changing the temperature signal amplitude, time of flight and velocity can change. For instance, Abbas et al. (Abbas and Shafiee 2018) generated wave velocity function for guided wave group velocity evaluation considering frequency and temperature effect. It was found that the function can be used at the temperature which is not higher than 130 °C, since, further temperature increase influences on the bonding characteristics of the sensors. However, the relation between temperature and the output of GWSHM is not linear, since, many factors caused by temperature variation influence on the guided waves. Changed stiffness of the materials has the impact on group and phase velocity; change of

elastic and shear moduli leads to longitudinal and transverse velocitites change resulting the decrease of phase velocity of the waves. As a result, in the case of temperature increase the propagating signals arrive later compared to temperature decrease. Expansion and contraction effect can lead to a change of distance between sensors and actuators, additionally, temperature variation has an impact on sensor properties and bonding layer properties (thickness and shear modulus) (Gorgin et al. 2020). Some numerical investigations presented a high impact of the temperature on the propagation of guided waves due to the change of physical properties.

If baseline subtraction technique described in previous section is used to detect structural changes, temperature compensation strategies is a must in order to minimise the residuals caused by environmental factors and to be able to detect smaller defects. Compensation techniques like optimal baseline subtraction (OBS), cointegration or baseline signal stretch (BSS) exist to reduce the influence of temperature to guided wave signals (Croxford et al. 2010; Gorgin et al. 2020; Konstantinidis et al. 2007). A comprehensive study on the influence of temperature to reflection, transmission and velocity of guided waves was recently presented by Abbas et al. (Abbas et al. 2020). In the case of OBS temperature compensation technique the baseline signals are measured over the temperature range whereupon the best matched baseline signal is selected according to subtract from any further reading from the structure. This technique requires large number of baseline signals each at different environmental condition and high temperature resolution. BSS temperature compensation technique is based on model building of the effects on wave signals due to temperature change. The shape change of the signals over the time is calculated (stretch factor) in order to perform time-stretch estimation (dilation or compression of the signal). This method works well for small temperature differences between baseline and current signal, however it's performance deteriorates at sufficiently large temperature differences (Croxford et al. 2007). Clarke et al. proposed to use a combination of OBS and BSS methods to reduce amount of baseline signals describing different temperature regimes (Clarke et al. 2010). In most cases, it's considered, that wave velocity is most important factor that changes with variation of temperature. However, recent studies show, that phase and amplitude of the signal are temperature sensitive as well. Changes in the temperature may cause variation of bonding stiffness between the sensor and the structure. This may alter the frequency response of transducer and lead to phase delay in the signal. Fendzi et al. proposed temperature compensation method that estimates linear dependencies of amplitude and phase delay versus temperature for each transducer pair mounted on the structure (Fendzi et al. 2016). Based on derived amplitude and phase factors, the regression model is then estimated and signal can be reconstructed at selected temperature. Recently Herdovics et al. proposed temperature compensation method which uses two sensors in close proximity only, hence the phase changes are compensated according to the incident wave, while the wave velocity changes are supressed from echoes. (Herdovics and Cegla 2019). The authors concluded that proposed compensation technique is able to reduce effect of environmental conditions from 7 dB to 20 dB in comparison to conventional single stretch BSS method at temperature difference of 41.5 °C between signals. Mariani

et al. presented a method for temperature compensation that takes into the account both velocity and phase information (Mariani et al. 2020). The main difference is that the later method provides estimate solely based on baseline and subsequent signals. The method demonstrated 97% POD for 0.1% probability of false alarm when the temperature difference ranges were between 7 °C to 28 °C and 35 °C to 55 °C. Meanwhile at the same conditions, standard BSS yielded up to 23% POD only.

Propagation of guided waves, also, can be affected by operational conditions which include vibration, loads and sensor bonding. Vibration can lead to interpretation complexity of structural behavior. The load applied on the structure can change a isotropic medium into an anisotropic medium, effective elastic constants lose symmetry, cause time-shift and phase velocity changes. To compensate the effect of load, the changes of phase shift and signal amplitude have to be taken into account. Additionally, sensor degradation occurs due to mechanical loading leading to piezoceramic transducer deterioration. In order to identify degradation mode as transducer disbonding the electromechanical impedance spectrum is determined by the electrical and the mechanical properties of the transducer and host structure which includes the adhesive line (Rajic et al. 2011). In order to ensure reliable performance of SHM system the influence of mechanical loading on the sensors, which cause its degradation, has to be reduced. The compensation strategy implies the use of specific element as a structural augmentation which is placed between transducer and the structure. As a result, the stresses in transducers caused by loading are reduced (Rajic et al. 2011).

5.4.4 POD Assessment Solutions

Comparing to NDE techniques which produce independent observation the data received from SHM system is dependent due to continuous data collection. Despite the fact that uncertainty factors of NDE and SHM differ, the same mathematical framework is applied for both systems (Gianneo et al. 2016). Guided waves provide fast and cost-effecive evaluation of different damage types compared to other approaches of SHM system. GWSHM has several indicators allowing to detect defects in the structure: changes in natural frequencies, in time of flight, in strain, in time domain signal and other characteristics. In order to evaluate POD of SHM system it is necessary to cover all sources of variability. As it was mentioned above, there are two configurations to assess POD—signal response and Hit/Miss. PFA has to be evaluated for SHM system due to high possibility of false calls (De Luca et al. 2020).

Mandache et al. (Mandache et al. 2011) described time-based POD assessment of SHM system. In comparison to NDE, SHM detects time evolution of the defect with respect to baseline signal. Therefore, POD can be defined not as a function of the defect size, but as a function of time it takes until the damage of certain size is firstly detected or a damage growth on pre-defined percentage. This approach was

proposed by Pollock who investigated the probability of detection of growing crack using acoustic emission. The crack of 4mm was growing to 4.05 mm and detected with a probability of 90% within 6 weeks of monitoring. Shorter period of monitoring time gives lower probability in the case of same crack (Mandache et al. 2011). Another approach to estimate POD of SHM system is to transfer POD from NDT to SHM. Firstly, POD assessment for NDT technique is performed. Then using transfer function where all influencing parameters are taken into account the POD is converted to POD curve equivalent to SHM system. One more alternative is to analyse two parallel structures under similar conditions periodically with NDT and continuously with SHM. The relationship of signal responses to damage between two systems is transferred to the POD curves, assuming that POD of NDT is known (Mandache et al. 2011).

Gianneo et al. (Gianneo et al. 2016) investigated Multi Parameter POD approach for guided waves of SHM. This approach implies the combination of Finite Element numerical simulations and experimental data to receive required POD curve. The combination of numerical and experimental data establishes "Measured â vs. Modelled a" data diagram considering influencing factors and uncertain parameters. As a result, non-linear responses of the GWSHM system is being linearized by the diagram allowing the use of Berens' statistical model. Then a POD curve is estimated as a function of modelling data. Multi-Dimensional POD implies the analysis of SHM system responses as a function of damage size with the influence of factors and isolate the recorded signals that are sensitive only to a single influencing factor, including damage. After POD curves of damage size for each independent influencing factor are found then POD fusion of these curves can be performed. Therefore, SHM reliability in the presence of combined influencing factors can be determined (Mandache et al. 2011).

5.4.5 Model-Assisted POD for SHM System

Large scale of experiments are required in order to evaluate POD of the system. A number of repetitive tests has to be performed for the same crack size to take in consideration the uncertainty of influencing factors. This approach of POD evaluation is time-consuming and expensive. Thus, Model Assisted POD (MAPOD) was developed as a solution of the problem (Gallina et al. 2013).

Alfredo et al. states that the support of numerical simulations is required for POD assessment. Verification and validation method of the SHM system has to evaluate all aspects which can influence on detection capability, localization and characterization of the defect as well as an effect of environment and exploitation over time. Since sensors of SHM system are fixed at the same position the main difficulty is that the flaw may occur anywhere what will cause the change in response due to distance between sensors and defect. As a result, model for guided waves SHM system POD assessment is proposed and shown in Fig. 5.6 (Güemes et al. 2020).

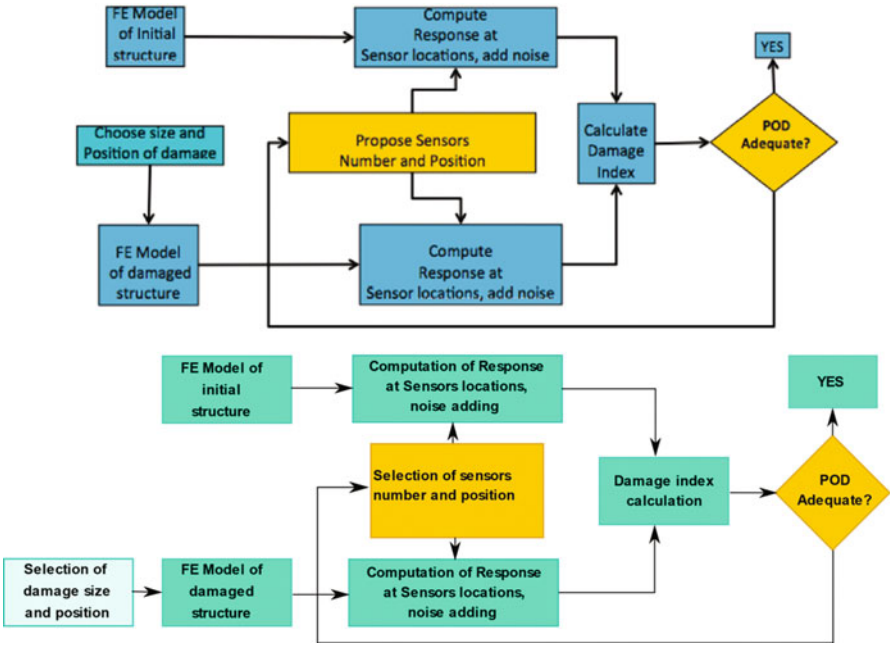

Fig. 5.6 Algorithm used to calculate POD of SHM system (Güemes et al. 2020)

Mainly, there are two MAPOD approaches of high interest: transfer function and full model assisted. Transfer function approach is physics based and used to transfer POD of specific inspection to another with different parameters of inspection. Full model assisted approach is based on the models of uncertainty propagation of specified inspection parameters. Numerical signal of the approach is combined with experimental noise. Nowadays, the use of computer models to evaluate the reliability of SHM system is the most suitable approach. MAPOD reduces experimental inspections of the samples by modelling responses of inspection of the defected material. In the case of effective MAPOD calculations enhance statistical models have to be created. These statistical models characterize system dependency on various influencing factors including defect. Additionally, the polynomial chaos methods reduce the number of samples required for assessment and speed up the MAPOD as well as parallel computing techniques greatly cut down the time of simulations (Gallina et al. 2013; Mandache et al. 2011).

Gallina et al. (Gallina et al. 2013) proposed the MAPOD approach to analyze the Lamb wave SHM system. Propagation signals received by the sensors were collected. Then the effect of dispersion was eliminated by the linear mapping algorithm. All signals were delayed and summed. Location and detection of the damage was performed using imagining technique. Numerical experiments were modelled and empirical white Gaussian noise was added to the recorded signals of sensors for consideration of in-situ factors. The data of simulated experiments was used in statistical analysis for POD curve and PFA evaluation.

Additional example of MAPOD evaluation of SHM systems is described. Cobb et al. (Cobb et al. 2009) proposes hit/miss configuration and model assisted approach for POD estimation of SHM system. Proposed model assisted approach comprises a creation of a series of models:

- Measurement response model which approximates the sensor response;
- Defect propagation model in order to generate sensor responses using a crack growth equation;
- Detection strategy to determine when damage is detected.

After, Hit/Miss analysis of resulting data was performed. Logistics regression was used for modelling binomial response data. POD curve was evaluated and indicates the percentage of all defects of specific size which will be detected (Cobb et al. 2009).

5.5 Guided Wave Applications to SHM of Aerospace Components

The purpose of structural health monitoring is to increase operational safety of aircrafts (Diamanti and Soutis 2010). Ultrasonic guided waves can be exploited for the structural health monitoring of large-scale plate-like aircraft structures (Staszewski et al. 2009). Although there have been investigations for application of the guided waves for metallic and composite aircraft components and structures, guided waves were mostly used up to now for the investigation of the simpler structures, such as pipes (Cawley 2018). In case of most aircraft components, the structures to be inspected have much more complex geometry, including stiffeners and bolt holes, what complicates the propagation of guided waves and thus the inspection. Below, some possible applications of guided waves for the inspection of the most frequently found defect types in the metallic and composite aerospace components as well as adhesive joints are reviewed.

Bae et al. (Bae and Lee 2016) and Choi et al. (Choi et al. 2018) have used serially connected PZT sensor net in combination with laser ultrasonic propagation imaging system for fatigue crack detection in metallic fuselage of Cessna 150 (Bae and Lee 2016). Using finite element modelling Ewald et al. investigated transducer placement for detections of cracks in aluminum aircraft structures using the Lamb wave SHM system (Ewald et al. 2018). Masserey et al. (Masserey and Fromme 2015) have used high frequency 2.25MHz Lamb waves for the monitoring of fatigue crack growth in aluminum specimens. Ihn et al. (Ihn and Chang 2008) have proposed to use an imaging method for quantification of damage in aluminum structures using multiple pitch-catch information. Dalton et al. (Dalton et al. 2001) concluded that guided waves could be used for localized monitoring of metallic airframe structures up to 1 m, however they are not feasible for the monitoring of complete fuselages.

Chang et al. investigated corrosion monitoring using Lamb wave tomography in aluminum plate (Chang et al. 2020). 15 pairs of PZT sensors were used for the excitation and reception of Lamb waves. As A_0 mode is more sensitive to variations in the thickness, it was used for the corrosion monitoring (Chang et al. 2020).

Fakih et al. have used piezoelectric wafers for the excitation of S_0 mode Lamb waves for assessment of flaws in frictions stir welded joints (Fakih et al. 2018). The proposed approach was verified by computed tomography as in the research of Jasiuniene et al. investigating the quality of dissimilar metal joints made by friction stir welding (Jasiūnienė et al. 2017).

Huan et al. suggest using a shear horizontal SH guided wave based SHM system with total focusing method imaging for monitoring of metallic structures (Huan et al. 2019). The suitability of the shear horizontal waves for the defect detection in metallic structures was investigated as well by Petcher et al. (Petcher and Dixon 2015).

The composite materials are used in different aircraft primary structures more and more (Diamanti and Soutis 2010). The most common type of damage is caused by impact, which can cause delaminations, disbonds, matrix cracking, fiber breakage leading to the reduction of structure's life (Diamanti and Soutis 2010).

Impact type of damage was investigated using Lamb waves by different authors: Diamanti et al. have used lamb waves (A_0 mode) for detection and localization of impact damage in composite beams (Diamanti and Soutis 2010); Their investigations have proved that Lamb waves can be used to monitor impact damage evolution in composite laminated structures (Diamanti and Soutis 2010). However, it was concluded, that for application in situ there are still some issues to be solved: durability of bonding layer between the transducer and structure, influence of environmental conditions, etc. (Diamanti and Soutis 2010). Memmolo et al. (2018a, 2018b) have used permanently installed sensors and developed an algorithm using multi-parameter approach to identify hidden flaws due to impact type of damage in composite structure. They have obtained promising results even in the areas with stiffeners and holes (Memmolo et al. 2018a). Katunin et al. have used embedded PZT sensors for detection of barely visible impact damage in GFRP and hybrid Al-GFRP-Al structures (Katunin et al. 2015). They have concluded, that low number of PZT sensors gives only rough image of inspected composite structure and could be used only as initial step of inspection (Katunin et al. 2015). Khodaei et al. (Sharif Khodaei and Aliabadi 2016) have proposed a multi-level approach for barely visible impact damage detection, identification and localization. Their results show that the number and location of the transducers influence the reliability of the detection. Capriotti et al. (2017) have used non-contact air coupled transducers for the generation of guided waves and detection of impact damage (causing cracked skin/stringer and disbonded stringer) in composite aircraft panels.

Lamb waves can also be used for finding of delamination type of defects in composites: Ramadas et al. (Ramzi et al. 2015) have studied the interaction of guided Lamb waves with an asymmetrically located delamination in laminated composite plate. Staszewski et al. (2009) used Lamb waves to detect delamination in the composite plate. One piezo ceramic actuator was used for Lamb wave generation,

and 3D laser vibrometer for reception (Staszewski et al. 2009). Ihn et al. (Ihn and Chang 2008) have used diagnostic imaging method using multiple pitch-catch pairs to quantify the delamination type damage in stiffened composite panels. Qiu et al. (2013) have used PZTs bonded to the structure with advanced two step signal processing for the localization of damage in composite wing panels with stiffeners and bolt holes. Kazys et al. (Kažys et al. 2006; Kazys et al. 2006) have detected delamination and impact type defects using air-coupled excitation of Lamb waves in aerospace honeycomb structures. A study on delamination size and depth extraction on composite plate using A_0 mode was presented by Samaitis et al. (2020, Tiwari et al. (2017).

Panda et al. for excitation and receiving of Lamb waves in composite aileron used air-coupled transducers in pitch catch mode (Panda et al. 2016) and have determined, that fundamental A_0 mode was effective for disbond detection (Panda et al. 2016). In another experiment by Panda et al. (2018) again air coupled transducers were used in pitch-catch configuration for generation and reception of A_0 Lamb wave mode in composite panel with stiffeners for disbond detection. Memmolo et al. (2018c) and Monaco et al. (2016) have investigated the possibilities to detect disbond of stringers in stiffened composites typically used for wing boxes using scattered guided waves and tomographic approach.

Adhesively bonded joints are attractive in aircraft structures as alternative to rivets. However, the degradation of the quality of adhesive joints is still an issue. Yilmaz et al. (Yilmaz and Jasiūnienė 2020) have suggested the techniques for detection of weak composite-adhesive joints using advanced NDT. Castaings (2014) have used the SH guided waves for the evaluation of the adhesion in adhesively bonded aluminum lap joints.

Especially challenging for the inspection are adhesive hybrid metal to composite joints. Advanced ultrasonic testing with novel signal post processing technique was suggested by Jasiūnienė et al. (2019) for detection of defect in the complex joints. Puthillath et al. (Puthillath and Rose 2010) have used ultrasonic guided wave modes with large in-plane displacement at the interface for the inspection of adhesively bonded aircraft repair patch (titanium repair patch bonded to an aluminum aircraft skin). Ren et al. (Ren and Lissenden 2013) also have used ultrasonic guided wave mode with large in-plane displacement at interface for the inspection of adhesive bonds between composite laminates.

Even though there has been a lot of different research of possible SHM application for different aircraft structures in the laboratory conditions, there haven't been a lot applications on real aircrafts due to several unsolved issues (Cawley 2018; Qing et al. 2019) like sensitivity of the SHM systems to environmental changes (Kralovec and Schagerl 2020; Gorgin et al. 2020; Abbas et al. 2020; Fang et al. 2019; Nokhbatolfoghahai et al. 2021), leading to reduced reliability (Memmolo et al. 2018a; Fang et al. 2019) and thus probability of the detection (Meeker et al. 2019; Wu et al. 2015), legal issues and other. Quantification of the extent of the damage as well remains a challenge (Ihn and Chang 2008). Another issue, which still haven't got enough attention is the huge amount of data to be analyzed (Qing et al. 2019). Effect of damaged/inoperative sensors also should be solved introducing self

diagnostic approach (Memmolo et al. 2018a; Qing et al. 2019). On the other hand, weight of the SHM system should be also not forgotten (Memmolo et al. 2018a)—additional weight introduced due to SHM system should be as low as possible.

5.6 Summary

The production of the modern aircraft clearly seeks faster, cheaper production, increased automation, reduced weight and fuel consumption. Modern aircraft manufacturing technologies use resin transfer molding (RTM), high pressure HP-RTM, thermoplastic composites, hybrid metal-composite structures and 3D printed parts (Composites World 2019). For example, HP-RTM are already implemented in some parts of an aircraft, allowing to achieve approx. 30% cost reduction and increase of the production efficiency by 10–20% (Composites World 2019). Thermoplastic composite technology will reduce the amount of assembly steps, eliminate some rivets and fasteners, resulting in reduced overall manufacturing cost. AM technologies, like the ones used in GE9X engine, allow to reduce weight of the engine and to combine multiple parts into single one overcoming the shape restrictions that come from conventional methods such as stamping and casting (Kellner 2020; Bachmann et al. 2017). Boeing is in production of 777X aircraft and in the design stage of New Midsize Aircraft (NMA or 797). Airbus is aiming to replace it's most successful single aisle jet A320 with a new A321XLR. New and modern jet's will increasingly use advanced manufacturing technologies, like the ones mentioned above. As these drastically change the design process, the NDT technologies will have to adapt. New knowledge of guided wave interaction with thermoplastic composite joints (Ochôa et al. 2019; Ochôa et al. 2018), HP-RTM components, detection of porosity or lack of fusion between layers of AM parts (Honarvar and Varvani-Farahani 2020) will be a key factor determining the inspection quality. The new NDT technologies will be required to overcome current limitations and provide full characterization of the damage including size, location and depth. This is crucial for successful damage progression models, which are responsible for remaining life predictions of the structure. For example, it has been reported that the depth of delamination is directly related to the damage progression mechanisms (Canturri et al. 2013; Elliott Cramer 2018), so it has to be fully defined by the monitoring system. Different manufacturing processes and novel materials will require different characterization data and assessment of all defects that are present in the structure. The defects of different kinds will have to be described differently depending on their nature and progression mechanisms. Hence, the SHM system will have to be versatile and adaptive enought. Both in-service and production line inspection technologies will become crucial as they will determine the manufacturing rates and safety of new structural desings, while guided waves demonstrate a serious potential to become one of the key SHM technologies of the future aircraft.

References

Abbas M, Shafiee M (2018) Structural health monitoring (SHM) and determination of surface defects in large metallic structures using ultrasonic guided waves. Sensors 18:3958

Abbas S et al (2020) Experimental investigation of impact of environmental temperature and optimal baseline for thermal attenuation in structural health monitoring based on ultrasonic guided waves. Wave Mot 93:102474

Aldrin JC, Knopp JS, Sabbagh HA (2013) Bayesian methods in probability of detection estimation and model-assisted probability of detection evaluation. AIP Conf Proc 1511(1):1733–1740

Aldrin JC, et al. (2016) Best practices for evaluating the capability of nondestructive evaluation (NDE) and structural health monitoring (SHM) techniques for damage characterization. Available from <https://ui.adsabs.harvard.edu/abs/2016AIPC.1706t0002A>. ISBN 0094-243X

Alokita S et al (2019) Structural health monitoring of biocomposites, fibre-reinforced composites and hybrid composites. In: Jawaid, Mohammad; Thariq, Mohamed and Saba, Naheed (eds) 4 – Recent advances and trends in structural health monitoring, Woodhead Publishing, Cambridge, pp 53-73. Available from <http://www.sciencedirect.com/science/article/pii/B9780081022917000046>. Isbn 9780081022917

Alonso L, et al. (2018) Middleware and communication technologies for structural health monitoring of critical infrastructures: A survey. Comp Stand Interfaces 56:83-100.

Bachmann J, Hidalgo C, Bricout S (2017) Environmental analysis of innovative sustainable composites with potential use in aviation sector—a life cycle assessment review. Sci China Technol Sci 60:1301–1317

Bae DY, Lee JR (2016) A health management technology for multisite cracks in an in-service aircraft fuselage based on multi-time-frame laser ultrasonic energy mapping and serially connected PZTs. Aerospace Sci Technol 54:114–121. https://doi.org/10.1016/j.ast.2016.04.014

Barski M, Stawiarski A (2018) The crack detection and evaluation by elastic wave propagation in open hole structures for aerospace application. Available from <http://www.sciencedirect.com/science/article/pii/S1270963818302190>. ISBN 1270-9638

Belanger P, Cawley P (2009) Feasibility of low frequency straight-ray guided wave tomography. Available from <http://www.sciencedirect.com/science/article/pii/S0963869508001205>. ISBN 0963-8695

Belanger P, Cawleyand P, Simonetti F (2010) Guided wave diffraction tomography within the born approximation. ISBN 1525-8955

Bellan F, et al. (2005) A new design and manufacturing process for embedded lamb waves interdigital transducers based on piezopolymer film. Available from <http://www.sciencedirect.com/science/article/pii/S0924424705003468>. ISBN 0924-4247

Benmeddour F et al (2009) Experimental study of the A0 and S0 lamb waves interaction with symmetrical notches. Available from <http://www.sciencedirect.com/science/article/pii/S0041624X08001480>. ISBN 0041-624X

Birt EA (1998) Damage detection in carbon-fibre composites using ultrasonic Lamb waves. Insight 40(5):335

Caminero MA et al (2013) Analysis of adhesively bonded repairs in composites: damage detection and prognosis. Compos Struct 95:500–517

Canturri C et al (2013) Delamination growth directionality and the subsequent migration processes – the key to damage tolerant design. Compos Part A Appl Sci Manufact 54:79–87

Capriotti M et al (2017) Non-destructive inspection of impact damage in composite aircraft panels by ultrasonic guided waves and statistical processing. Materials 10(6):616

Castaings M (2014) SH ultrasonic guided waves for the evaluation of interfacial adhesion. Ultrasonics 54(7):1760–1775

Cawley P (2007) Practical guided wave inspection and applications to structural health monitoring. In: Proceedings of the 5th australasian congress on applied mechanics (ACAM 2007), Brisbane, Australia. ISBN 0858-258625

Cawley P (2018) Structural health monitoring: closing the gap between research and industrial deployment. Struct Health Monit 17(5):1225–1244. https://doi.org/10.1177/1475921717750047

Chang M, Yuan S, Guo F (2020) Corrosion monitoring using a new compressed sensing-based tomographic method. Ultrasonics 101:105988. https://doi.org/10.1016/j.ultras.2019.105988

Chapuis B, Calmon P, Jenson F (2018a) Best practices for the use of simulation in POD curves estimation: application to UT weld inspection. In: Chapuis B, Calmon P, Jenson F (eds) Basics of statistics for POD. Springer International Publishing, Cham, pp 25–32. https://doi.org/10.1007/978-3-319-62659-8_8. isbn:978-3-319-62659-8

Chapuis B, Calmon P, Jenson F (2018b) Best practices for the use of simulation in POD curves estimation. Springer International Publishing, Cham. isbn:978-3-319-62658-1

Chen J, Yuan S, Jin X (2019) On-line prognosis of fatigue cracking via a regularized particle filter and guided wave monitoring. Available from <http://www.sciencedirect.com/science/article/pii/S0888327019303309>. ISBN 0888-3270

Choi Y, Abbas SHL, Jung R (2018) Aircraft integrated structural health monitoring using lasers, piezoelectricity, and fiber optics. Meas J Int Meas Conf 125:294–302. https://doi.org/10.1016/j.measurement.2018.04.067

Clarke T, Simonetti F, Cawley P (2010) Guided wave health monitoring of complex structures by sparse Array systems: influence of temperature changes on performance. J Sound Vib 329 (12):2306–2322

Cobb A, Michaels J, Michaels T (2009) Ultrasonic structural health monitoring: a probability of detection case study, vol 1096

Composites World (2019) Next-gen aerospace: advanced materials and processes. Available from <https://gbmsupplements.mydigitalpublication.com/publication/?i=587161&p=&pn=>

Croxford AJ et al (2007) Strategies for guided-wave structural health monitoring. Proc R Soc Lond A Math Phys Eng Sci 463(2087):2961–2981

Croxford AJ et al (2010) Efficient temperature compensation strategies for guided wave structural health monitoring. Ultrasonics 50(4–5):517–528

Dai D, He Q (2014) Structure damage localization with ultrasonic guided waves based on a time–frequency method. Sig Process 96:21–28

Dalton RP, Cawley P, Lowe MJS (2001) The potential of guided waves for monitoring large areas of metallic aircraft fuselage structure. J Nondestruct Eval 20(1):29–46. https://doi.org/10.1023/A:1010601829968

Datteo A et al (2018) On the use of AR models for SHM: a global sensitivity and uncertainty analysis framework. Reliab Eng Syst Saf 170:99–115

De Luca A et al (2020) Guided wave SHM system for damage detection in complex composite structure. Theor Appl Fract Mec 105:102408

De Marchi L, Perelli A, Marzani A (2013) A signal processing approach to exploit chirp excitation in lamb wave defect detection and localization procedures. Available from <http://www.sciencedirect.com/science/article/pii/S0888327012003913>. ISBN 0888-3270

Department of Defense (2009) Nondestructive evaluation system reliability assessment. Department of Defense, United States of America

Diamanti K, Soutis C (2010) Structural health monitoring techniques for aircraft composite structures. Available from <https://ac.els-cdn.com/S0376042110000369/1-s2.0-S0376042110000369-main.pdf?_tid=5b5f4ba4-51f1-4802-a081-b6bcf08f71ee&acdnat=1521634767_e5a756ebeb7a134a9013ab38b619702f>. ISBN 0376-0421

Djili S, et al. (2013) Notch detection in copper tubes immersed in water by leaky compressional guided waves. Available from <http://www.sciencedirect.com/science/article/pii/S0963869512001417>. ISBN 0963-8695

Duong NT, et al. (2015) Relation between the ultrasonic attenuation and the porosity of a RTM composite plate. Available from <http://www.sciencedirect.com/science/article/pii/S1875389215007567>. ISBN 1875-3892

Ecke W (2000) Optical fibre grating strain sensor network for x-38 spacecraft health monitoring. Available from https://doi.org/10.1117/12.2302163

Elliott Cramer K (2018) Current and future needs and research for composite materials NDE. Available from doi:https://doi.org/10.1117/12.2291921

Etebu E, Shafiee M (2018) Reliability analysis of structural health monitoring systems, pp 2243–2247. ISBN 9781351174664

Ewald V, Groves R, Benedictus R (2018) Transducer placement option of Lamb wave SHM system for hotspot damage monitoring. Aerospace 5(2):39

Fakih MA et al (2018) Detection and assessment of flaws in friction stir welded joints using ultrasonic guided waves: experimental and finite element analysis. Mech Syst Sig Proces 101:516–534. https://doi.org/10.1016/j.ymssp.2017.09.003

Fan Z et al. (2013) Feature-guided waves for monitoring adhesive shear modulus in bonded stiffeners. Available from <http://www.sciencedirect.com/science/article/pii/S0963869512001673>. ISBN 0963-8695

Fang F et al (2019) Dynamic probability modeling-based aircraft structural health monitoring framework under time-varying conditions: validation in an in-flight test simulated on ground. Aerospace Sci Technol 95:105467

Fendzi C et al (2016) A data-driven temperature compensation approach for structural health monitoring using Lamb waves. Struct Health Monit 15(5):525–540. https://doi.org/10.1177/1475921716650997

Feng B, Ribeiro AL, Ramos HG (2018) Interaction of lamb waves with the edges of a delamination in CFRP composites and a reference-free localization method for delamination. Available from <http://www.sciencedirect.com/science/article/pii/S0263224117306425>. ISBN 0263-2241

Fisher J, Michaels J (2009) Model-assisted probability of detection for ultrasonic structural health monitoring. In: 4th European American workshop on reliability of NDE, 2009

Fromme P et al (2006) On the development and testing of a guided ultrasonic wave array for structural integrity monitoring. IEEE Trans Ultrason Ferroelectr Freq Control 53(4):777–785

Fromme P, Reymondin J-P, Masserey B (2017) High frequency guided waves for disbond detection in multi-layered structures. Acta Acustica United Acustica 103:932–940

Gallina A, Paćko P, Ambroziński Ł (2013) Model assisted probability of detection in structural health monitoring.. Available from <https://doi.org/10.1002/9781118536148.ch3>. ISBN 9781-118536148

Gangadharan R et al (2009) Time reversal technique for health monitoring of metallic structure using Lamb waves. Ultrasonics 49(8):696–705

Gianneo A, Carboni M, Giglio M (2016) Reliability aspects and multi-parameter POD formulation for guided wave based SHM techniques

Giridhara G et al (2010) Rapid localization of damage using a circular sensor array and Lamb wave based triangulation. Mech Syst Signal Process 24(8):2929–2946

Giurgiutiu V (2005) Tuned lamb wave excitation and detection with piezoelectric wafer active sensors for structural health monitoring. J Intell Mater Syst Struct 16(4):291–305

Giurgiutiu V (2011) Structural damage detection with piezoelectric wafer active sensors. J Phys Conf Ser 305(1):012123

Giurgiutiu V (2015) 16 – Structural health monitoring (SHM) of aerospace composites. In: Irving PE, Soutis C (eds) Woodhead Publishing. Available from <http://www.sciencedirect.com/science/article/pii/B9780857095237000165>. ISBN 9780-857095237

Giurgiutiu V, Bao JJ (2004) Embedded-ultrasonics structural radar for in situ structural health monitoring of thin-wall structures. Struct Health Monit 3(2):121–140

Giurgiutiu V, Zagrai AB, Jingjing B (2004) Damage identification in aging aircraft structures with piezoelectric wafer active sensors. J Intell Mater Syst Struct 15(9–10):673–687

Glushkov EV et al (2010) Selective lamb mode excitation by piezoelectric coaxial ring actuators. Smart Mater Struct 19(3):035018

Gorgin R, Luo Y, Wu Z (2020) Environmental and operational conditions effects on Lamb wave based structural health monitoring systems: a review. Ultrasonics 105:106114. https://doi.org/10.1016/j.ultras.2020.106114

Grondel S et al (2002) Design of optimal configuration for generating A0 Lamb mode in a composite plate using Piezoceramic transducers. J Acoust Soc Am 112(1):84

Güemes A, et al. (2020) Structural health monitoring for advanced composite structures: a review. ISBN 2504-477X

Hauffe A, Hähnel F, Wolf K (2020) Comparison of algorithms to quantify the damaged area in CFRP ultrasonic scans. Available from <http://www.sciencedirect.com/science/article/pii/S0263822319336153>. ISBN 0263-8223

Hellier C (2012) Handbook of nondestructive evaluation, 2nd edn. McGraw-Hill Professional, New York

Herdovics B, Cegla F (2019) Compensation of phase response changes in ultrasonic transducers caused by temperature variations. Struct Health Monit 18(2):508–523. https://doi.org/10.1177/1475921718759272

Higgins A (2000) Adhesive bonding of aircraft structures. Int J Adhes Adhes 20(5):367–376

Honarvar F, Varvani-Farahani A (2020) A review of ultrasonic testing applications in additive manufacturing: defect evaluation, material characterization, and process control. Ultrasonics 108:106227

Hsu, D. K. (2013) 15 – Non-destructive evaluation (NDE) of aerospace composites: ultrasonic techniques. In: Karbhari, Vistasp M (ed) Non-destructive evaluation (NDE) of polymer matrix composites. Woodhead Publishing, Cambridge. Available from <http://www.sciencedirect.com/science/article/pii/B9780857093448500154>. ISBN 9780-857093448

Hu N, et al. (2008) Identification of delamination position in cross-ply laminated composite beams using S0 Lamb mode. Available from <http://www.sciencedirect.com/science/article/pii/S0266353807004113>. ISBN 0266-3538

Huan Q et al (2019) A high-resolution structural health monitoring system based on SH wave piezoelectric transducers phased array. Ultrasonics 97:29–37

Ihn J-B, Chang F-K (2008) Pitch-catch active sensing methods in structural health monitoring for aircraft structures. Struct Health Monit 7(1):5–19. https://doi.org/10.1177/1475921707081979

Ito J, et al. (2015) Ultrasonic wave propagation in the corner section of composite laminate structure: numerical simulations and experiments. Available from <http://www.sciencedirect.com/science/article/pii/S0263822314006825>. ISBN 0263-8223

Jasiūnienė E et al (2017) Investigation of dissimilar metal joints with nanoparticle fillers. NDT E Int 92:122–129

Jasiūnienė E et al (2019) Ultrasonic non-destructive testing of complex titanium/carbon fibre composite joints. Ultrasonics 95:13–21

Jayaraman C, Chitti Venkata K, Balasubramaniam K (2009) Higher order modes cluster (Homc) guided waves-a new technique for ndt inspection. In: AIP conference proceedings, vol 1096

Jin J, Quek ST, Wang Q (2005) Design of interdigital transducers for crack detection in plates. Ultrasonics 43(6):481–493

Jurek M, et al. (2018) Non-contact excitation and focusing of guided waves in CFRP composite plate by air-coupled transducers for application in damage detection. Available from <http://www.sciencedirect.com/science/article/pii/S2452321618304384>. ISBN 2452-3216

Kabban S, Christine M et al (2015) The probability of detection for structural health monitoring systems: repeated measures data. Struct Health Monitor 14(3):252–264

Katunin A, Dragan K, Dziendzikowski M (2015) Damage identification in aircraft composite structures: a case study using various non-destructive testing techniques. Compos Struct 127:1–9. https://doi.org/10.1016/j.compstruct.2015.02.080

Kažys R et al (2006) Air-coupled ultrasonic investigation of multi-layered composite materials. Ultrasonics 44:e819–e822

Kazys R, et al. (2006) Ultrasonic air-coupled non-destructive testing of aerospace components. pp 1–8. Available from <https://www.ndt.net/article/ecndt2006/doc/We.1.1.5.pdf

Kazys JR, Sliteris R, Sestoke J (2017) Air-coupled ultrasonic receivers with high electromechanical coupling PMN-32%PT strip-like piezoelectric elements. Sensors 17(10):2365

Kellner T (2020) The next generation: a team of young engineers helped bring 3D printing inside the World's largest jet engine. Available from <https://www.ge.com/news/reports/the-next-generation-this-team-of-young-engineers-helped-bring-3d-printing-inside-the-worlds-largest-jet-engine>

Khalili P, Cawley P (2018) The choice of ultrasonic inspection method for the detection of corrosion at inaccessible locations. NDT & E Int 99:80–92

Kijanka P, Staszewski WJ, Packo P (2018) Generalised semi-analytical method for excitability curves calculation and numerical modal amplitude analysis for lamb waves. Struct Contr Health Monit 25(7):e2172

Kim K-B, Hsu DK, Barnard DJ (2013) Estimation of porosity content of composite materials by applying discrete wavelet transform to ultrasonic backscattered signal. Available from <http://www.sciencedirect.com/science/article/pii/S0963869513000212>. ISBN 0963-8695

Konstantinidis G, Wilcox PD, Drinkwater BW (2007) An investigation into the temperature stability of a guided wave structural health monitoring system using permanently attached sensors. IEEE Sens J 7(5):905–912

Kralovec C, Schagerl M (2020) Review of structural health monitoring methods regarding a multi-sensor approach for damage assessment of metal and composite structures. ISBN 1424-8220

Kudela P, Ostachowicz W, Żak A (2008) Damage detection in composite plates with embedded PZT transducers. Mech Syst Signal Process 22(6):1327–1335

Lamb H (1917) On waves in an elastic plate. Proc R Soc Lond Ser A Containing Papers Math Phys Character 93(648):114–128

Lee TH, Choi IH, Jhang KY (2008) Single-mode guided wave technique using ring-arrayed laser beam for thin-tube inspection. Available from <http://www.sciencedirect.com/science/article/pii/S0963869508000340>. ISBN 0963-8695

Li S, et al. (2016) Leak detection and location in gas pipelines by extraction of cross spectrum of single non-dispersive guided wave modes. Available from <http://www.sciencedirect.com/science/article/pii/S0950423016302650>. ISBN 0950-4230

Li L et al (2019) Sensor fault detection with generalized likelihood ratio and correlation coefficient for bridge SHM. J Sound Vib 442:445–458

Lin L et al (2011) A novel random void model and its application in predicting void content of composites based on ultrasonic attenuation coefficient. Appl Phys A 103(4):1153–1157

Long R, Lowe M, Cawley P (2003) Attenuation characteristics of the fundamental modes that propagate in buried iron water pipes. Ultrasonics 41(7):509–519

Luo Z et al (2016) A reshaped excitation regenerating and mapping method for waveform correction in lamb waves dispersion compensation. Smart Mater Struct 26(2):025016

Majumder M, et al. (2008) Fibre bragg gratings in structural health monitoring—present status and applications. Available from <http://www.sciencedirect.com/science/article/pii/S0924424708002380>. ISBN 0924-4247

Mandache C, et al. (2011) Considerations on structural health monitoring reliability. [cited 5 Aug 2020]

Mardanshahi A et al (2020) Detection and classification of matrix cracking in laminated composites using guided wave propagation and artificial neural networks. Available from <http://www.sciencedirect.com/science/article/pii/S0263822319345684>. ISBN 0263-8223

Mariani S, Heinlein S, Cawley P (2020) Compensation for temperature-dependent phase and velocity of guided wave signals in baseline subtraction for structural health monitoring. Struct Health Monit 19(1):26–47. https://doi.org/10.1177/1475921719835155

Masserey B, Fromme P (2015) In-situ monitoring of fatigue crack growth using high frequency guided waves. NDT & E Int 71:1–7

Masserey B, Raemy C, Fromme P (2014) High-frequency guided ultrasonic waves for hidden defect detection in multi-layered aircraft structures. Ultrasonics 54(7):1720–1728
Mazzotti M, Marzani A, Bartoli I (2014) Dispersion analysis of leaky guided waves in fluid-loaded waveguides of generic shape. Available from <http://www.sciencedirect.com/science/article/pii/S0041624X13001832>. ISBN 0041-624X
Meeker W, Roach D, Kessler S (2019) Statistical methods for probability of detection in structural health monitoring.
Melnykowycz M et al (2006) Performance of integrated active fiber composites in fiber reinforced epoxy laminates. Smart Mater Struct 15(1):204–212
Memmolo V, et al. (2018a) Damage localization in composite structures using a guided waves based multi-parameter approach. ISBN 2226-4310
Memmolo V, Pasquino N, Ricci F (2018b) Experimental characterization of a damage detection and localization system for composite structures. Measurement 129:381–388
Memmolo V et al (2018c) Guided wave propagation and scattering for structural health monitoring of stiffened composites. Compos Struct 184:568–580
Michaels JE (2008) Detection, localization and characterization of damage in plates with anin situarray of spatially distributed ultrasonic sensors. Smart Mater Struct 17(3):035035. https://doi.org/10.1088/0964-1726/17/3/035035
Michaels JE 2016 Structural health monitoring (SHM) in aerospace structures. In: Yuan F-G (ed) 9 – Sparse array imaging with guided waves under variable environmental conditions, Woodhead Publishing, pp. 255-284. Available from <http://www.sciencedirect.com/science/article/pii/B9780081001486000093>. ISBN 9780081001486
Michaels JE, Michaels TE (2006) Enhanced differential methods for guided wave phased array imaging using spatially distributed piezoelectric transducers. AIP Conf Proc 820(1):837–844
Michaels JE, Michaels TE (2007) Guided wave signal processing and image fusion for in situ damage localization in plates. Wave Motion 44(6):482–492
Mitra M, Gopalakrishnan S (2016) Guided wave based structural health monitoring: a review. Smart Mater Struct 25(5):053001
Monaco E, et al. (2016) Methodologies for guided wave-based SHM system implementation on composite wing panels: results and perspectives from SARISTU Scenario, vol 5. pp 495-528. ISBN 978-3-319-22412-1
Monkhouse RSC et al (2000) The rapid monitoring of structures using interdigital lamb wave transducers. Smart Mater Struct 9(3):304
Munian RK, Roy Mahapatra D, Gopalakrishnan S (2020) Ultrasonic guided wave scattering due to delamination in curved composite structures. Available from <http://www.sciencedirect.com/science/article/pii/S0263822319339169>. ISBN 0263-8223
Mustapha S, Ye L (2014) Leaky and non-leaky behaviours of guided waves in CF/EP Sandwich structures. Wave Motion 51(6):905–918
Mustapha S, Ye L (2015) Propagation behaviour of guided waves in tapered sandwich structures and debonding identification using time reversal. Wave Motion 57:154–170
Nazeer N, Ratassepp M, Fan Z (2017) Damage detection in bent plates using shear horizontal guided waves. Ultrasonics 75:155–163
Nokhbatolfoghahai A, Navazi HM, Groves RM (2021) Evaluation of the sparse reconstruction and the delay-and-sum damage imaging methods for structural health monitoring under different environmental and operational conditions. Measurement 169:108495
Ochôa P et al (2018) Experimental assessment of the influence of welding process parameters on Lamb wave transmission across ultrasonically welded thermoplastic composite joints. Mech Syst Sig Process 99:197–218
Ochôa P et al. (2019) Diagnostic of manufacturing defects in ultrasonically welded thermoplastic composite joints using ultrasonic guided waves. Available from <http://www.sciencedirect.com/science/article/pii/S0963869518306017>. ISBN 0963-8695

Packo P et al (2016) Amplitude-dependent lamb wave dispersion in nonlinear plates. J Acoust Soc Am 140(2):1319–1331

Pain D, Drinkwater BW (2013) Detection of fibre waviness using ultrasonic array scattering data. J Nondestruct Eval 32(3):215–227

Panda RS, Rajagopal P, Balasubramaniam K (2016) Rapid ultrasonic inspection of stiffened composite ailerons. Available from <http://www.ultrangroup.com/

Panda RS, Rajagopal P, Balasubramaniam K (2018) Rapid guided wave inspection of complex stiffened composite structural components using non-contact air-coupled ultrasound. Available from <http://www.sciencedirect.com/science/article/pii/S0263822318321305>. ISBN 0263-8223

Papantoniou A, Rigas GA, Nikolaos D (2011) Assessment of the Strain Monitoring Reliability of Fiber Bragg Grating Sensor (FBGs) in advanced composite structures. Compos Struct 93 (9):2163–2172

Park HW, Kim SB, Sohn H (2009) Understanding a time reversal process in Lamb wave propagation. Wave Motion 46(7):451–467

Park J, et al. (2020) High-precision noncontact guided wave tomographic imaging of plate structures using a DHB algorithm. ISBN 2076-3417

Pelivanov, Ivan, et al. (2014) NDT of fiber-reinforced composites with a new fiber-optic pump–probe laser-ultrasound system. Available from <http://www.sciencedirect.com/science/article/pii/S2213597914000056>. ISBN 2213-5979

Petcher PA, Dixon S (2015) Weld defect detection using PPM EMAT generated shear horizontal ultrasound. NDT E Int 74:58–65. https://doi.org/10.1016/j.ndteint.2015.05.005

Podymova NB, et al. (2019) Laser-ultrasonic nondestructive evaluation of porosity in particulate reinforced metal-matrix composites. Available from <http://www.sciencedirect.com/science/article/pii/S0041624X19302707>. ISBN 0041-624X

Purekar AS et al (2004) Directional piezoelectric phased Array filters for detecting damage in isotropic plates. Smart Mater Struct 13(4):838

Puthillath P, Rose JL (2010) Ultrasonic guided wave inspection of a titanium repair patch bonded to an aluminum aircraft skin. Int J Adhes Adhes 30(7):566–573

Qing X, et al. (2019) Piezoelectric transducer-based structural health monitoring for aircraft applications. ISBN 1424-8220

Qiu L et al (2013) A quantitative multidamage monitoring method for large-scale complex composite. Struct Health Monit 12(3):183–196. https://doi.org/10.1177/1475921713479643

Raišutis R et al. (2010) Application of ultrasonic guided waves for non-destructive testing of defective CFRP rods with multiple delaminations. Available from <http://www.sciencedirect.com/science/article/pii/S0963869510000393>. ISBN 0963-8695

Rajic N, Tsoi KA, Rosalie C (2011) Issues on the durability of piezoceramic transducers for in situ SHM using acousto ultrasonics. [cited 5 Aug 2020]

Ramadas C et al (2009) Interaction of the primary anti-symmetric Lamb mode (Ao) with symmetric delaminations: numerical and experimental studies. Smart Mater Struct 18(8):085011

Ramadas C et al (2010) Interaction of guided Lamb waves with an asymmetrically located delamination in a laminated composite plate. Smart Mater Struct 19(6):065009

Ramzi AR, Mahmod MF, Elmi AB (2015) Immersion ultrasonic inspection system for small scaled composite specimen. J Eng Appl Sci 10:17146–17150

Ren B, Lissenden CJ (2013) Ultrasonic guided wave inspection of adhesive bonds between composite laminates. Int J Adhes Adhes 45:59–68

Rheinfurth, M., et al. (2011) Air-coupled guided waves combined with thermography for monitoring fatigue in biaxially loaded composite tubes. Available from <http://www.sciencedirect.com/science/article/pii/S026635381000480X>. ISBN 0266-3538

Rocha B et al (2013) New trends in structural health monitoring. In: Ostachowicz W, Güemes JA (eds) Structural health monitoring of aircraft structures, Vienna, Springer Vienna, pp 81–148. https://doi.org/10.1007/978-3-7091-1390-5_2. isbn:978-3-7091-1390-5

Römmeler A, et al. (2020) Air coupled ultrasonic inspection with lamb waves in plates showing mode conversion. Available from <http://www.sciencedirect.com/science/article/pii/S0041624X19303816>. ISBN 0041-624X
Rose JL (2002) A baseline and vision of ultrasonic guided wave inspection potential. J Pressure Vessel Technol 124(3):273–282
Rose JL (2004) Ultrasonic waves in solid media. Cambridge University Press. ISBN 978-0521548892
Rose JL (2014) Ultrasonic guided waves in solid media. Cambridge University Press. Available from https://doi.org/10.1017/CBO9781107273610. ISBN 9781107273610
Salas KI, Cesnik CES (2009) Guided wave excitation by a CLoVER transducer for structural health monitoring: theory and experiments. Smart Mater Struct 18(7):075005
Samaitis V, Mažeika L (2017) Influence of the spatial dimensions of ultrasonic transducers on the frequency spectrum of guided waves. ISBN 1424-8220
Samaitis V, Mažeika L, Rekuvienė R (2020) Assessment of the length and depth of delamination-type defects using ultrasonic guided waves. ISBN 2076-3417
Schaal C et al (2017) An analytical study of the scattering of ultrasonic guided waves at a delamination-like discontinuity in a plate. Proc Inst Mech Eng C J Mech Eng Sci 231 (16):2947–2960
Schoefs F, Abraham O, Popovics JS (2012) Quantitative evaluation of contactless impact echo for non-destructive assessment of void detection within tendon ducts. Constr Build Mater 37:885–892
Senyurek VY (2015) Detection of cuts and impact damage at the aircraft wing slat by using Lamb wave method. Measurement 67:10–23
Seung BK, Hoon S (2007) Instantaneous reference-free crack detection based on polarization characteristics of piezoelectric materials. Smart Mater Struct 16(6):2375
Sharif Khodaei Z, Aliabadi M (2016) A multi-level decision fusion strategy for condition based maintenance of composite structures. Materials 9(9):790
Shkerdin G, Glorieux C (2004) Lamb mode conversion in a plate with a delamination. J Acoust Soc Am 116(4):2089–2100
Sohn H et al (2007) Combination of a time reversal process and a consecutiv outlier analysis for baseline-free damage diagnosis. J Intell Mater Syst Struct 18(4):335–346
Sol T et al. (2018) Nondestructive ultrasonic evaluation of additively manufactured. AlSi10Mg samples. Available from <http://www.sciencedirect.com/science/article/pii/S2214860418300484>. ISBN 2214-8604
Solie LP, Auld BA (1973) Elastic waves in free anisotropic plates. J Acoust Soc Am 54(1):50–65
Staszewski WJ, Mahzan S, Traynor R (2009) Health monitoring of aerospace composite structures – active and passive approach. Compos Sci Technol 69(11–12):1678–1685
Stolz C, Meisner C (2020) Challenges for SHM reliability and application in aerospace industry. Available from:<https://www.sto.nato.int/publications/STO%20Meeting%20Proceedings/STO-MP-AVT-305/$MP-AVT-305-KN2.pdf>
Su Z, Ye LLY (2006) Guided Lamb waves for identification of damage in composite structures: a review. J Sound Vib 295(3–5):753–780
Takeda S, Okabe Y, Takeda N (2002) Delamination detection in CFRP laminates with embedded small-diameter fiber bragg grating sensors. Compos A Appl Sci Manufact 33(7):971–980
Teramoto K, Rabbi MS, Khan TI (2015) Detection of sub-surface delamination based on the spatio-temporal gradient analysis over the A0-mode lamb wave fields. Available from <http://www.sciencedirect.com/science/article/pii/S1875389215008342>. ISBN 1875-3892
Tiwari KA, Raisutis R, Samaitis V (2017) Hybrid signal processing technique to improve the defect estimation in ultrasonic non-destructive testing of composite structures. ISBN 1424-8220
Towsyfyan H, et al. (2020) Successes and challenges in non-destructive testing of aircraft composite structures. Available from <http://www.sciencedirect.com/science/article/pii/S1000936119303474>. ISBN 1000-9361

Tsoi K, Rajic N (2008) Durability and acoustic performance of integrated piezoceramic transducer elements under cyclic loading. Mater Forum 33.
Vanniamparambil PA et al. (2015) An active–passive acoustics approach for bond-line condition monitoring in aerospace skin stiffener panels. Available from <http://www.sciencedirect.com/science/article/pii/S1270963815001005>. ISBN 1270-9638
Veidt M, Liew CK (2012) 17 – Non-destructive evaluation (NDE) of aerospace composites: structural health monitoring of aerospace structures using guided wave ultrasonics. In: Karbhari VM (ed) Woodhead Publishing. Available from <http://www.sciencedirect.com/science/article/pii/B9780857093448500178>. ISBN 9780-857093448
Veit G, Bélanger P (2020) An ultrasonic guided wave excitation method at constant phase velocity using ultrasonic phased array probes. Available from <http://www.sciencedirect.com/science/article/pii/S0041624X19303932>. ISBN 0041-624X
Viktorov IA (1967) Rayleigh and lamb waves physical theory and applications. Springer US. ISBN 978-1-4899-5683-5
Wandowski T, Malinowski P, Ostachowicz WM (2011) Damage detection with concentrated configurations of piezoelectric transducers. Smart Mater Struct 20(2):025002
Wandowski T, Malinowski PH, Ostachowicz WM (2016) Circular sensing networks for guided waves based structural health monitoring. Mech Syst Signal Process 66–67:248–267
Wang Y et al (2020) A piezoelectric sensor network with shared signal transmission wires for structural health monitoring of aircraft smart skin. Mech Syst Sig Process 141:106730
Wilcox PD (2003) A rapid signal processing technique to remove the effect of dispersion from guided wave signals. ISBN 1525-8955
Wilcox P, Lowe M, Cawley P (2001a) The effect of dispersion on long-range inspection using ultrasonic guided waves. NDT & E Int 34(1):1–9
Wilcox PD, Lowe MJS, Cawley P (2001b) Mode and transducer selection for long range lamb wave inspection. J Intell Mater Syst Struct 12(8):553–565
Willey CL, et al. (2014) Guided wave tomography of pipes with high-order helical modes. Available from <http://www.sciencedirect.com/science/article/pii/S0963869514000449>. ISBN 0963-8695
Wojtczak E, Rucka M (2021) Monitoring the curing process of epoxy adhesive using ultrasound and lamb wave dispersion curves. Mech Syst Signal Process 151:107397
Wu Z et al (2015) Validation and evaluation of damage identification using probability-based diagnostic imaging on a stiffened composite panel. J Intell Mater Syst Struct 26(16):2181–2195. https://doi.org/10.1177/1045389X14549873
Xu B, Giurgiutiu V (2007) Single mode tuning effects on Lamb wave time reversal with piezoelectric wafer active sensors for structural health monitoring. J Nondestruct Eval 26(2):123
Xu C-B, et al. (2018) A guided wave dispersion compensation method based on compressed sensing. Available from <http://www.sciencedirect.com/science/article/pii/S0888327017305265>. ISBN 0888-3270
Yi T-H, Li H-N (2012) Methodology developments in sensor placement for health monitoring of civil infrastructures. Int J Distrib Sens Netw 8(8):612726. https://doi.org/10.1155/2012/612726
Yilmaz B, Jasiūnienė E (2020) Advanced ultrasonic NDT for weak bond detection in composite-adhesive bonded structures. Int J Adhes Adhes 102:102675
Yu X et al. (2017) Feature guided wave inspection of bond line defects between a stiffener and a composite plate. Available from <http://www.sciencedirect.com/science/article/pii/S0963869517301883>. ISBN 0963-8695
Zhang Z, et al. (2020a) Ultrasonic detection and characterization of delamination and rich resin in thick composites with waviness. Available from <http://www.sciencedirect.com/science/article/pii/S0266353819328751>. ISBN 0266-3538

Zhang Z et al (2020b) Visualized characterization of diversified defects in thick aerospace composites using ultrasonic B-scan. Compos Commun 22:100435

Zhao X et al (2007) Active health monitoring of an aircraft wing with embedded piezoelectric sensor/actuator network: I. Defect detection, localization and growth monitoring. Smart Mater Struct 16(4):1208–1217. https://doi.org/10.1088/0964-1726/16/4/032

Zhao G et al. (2019) Detection and monitoring of delamination in composite laminates using ultrasonic guided wave. Available from <http://www.sciencedirect.com/science/article/pii/S0263822319310827>. ISBN 0263-8223

Zichuan F, Jiang WW, William MD (2018) Non-contact ultrasonic gas flow metering using air-coupled leaky lamb waves. Available from <http://www.sciencedirect.com/science/article/pii/S0041624X17310466>. ISBN 0041-624X